Title
Piezo1-Regulated Mechanotransduction Controls Flow-Activated Lymphatic Expansion

Journal
Circulation Research, 131(2)

ISSN
0009-7330

Authors
Choi, Dongwon
Park, Eunkyung
Yu, Roy P
et al.

Publication Date
2022-07-08

DOI
10.1161/circresaha.121.320565

Peer reviewed

HHS Public Access

Author manuscript

Circ Res. Author manuscript; available in PMC 2023 July 08.

Published in final edited form as:

Circ Res. 2022 July 08; 131(2): e2–e21. doi:10.1161/CIRCRESAHA.121.320565.

Piezo1-Regulated Mechanotransduction Controls Flow-Activated Lymphatic Expansion

Dongwon Choi[1,2], **Eunkyung Park**[1,2], **Roy P. Yu**[1], **Michael N. Cooper**[1], **Il-Taeg Cho**[1,2], **Joshua Choi**[1], **James Yu**[1], **Luping Zhao**[1,2], **Ji-Eun Irene Yum**[1,2], **Jin Suh Yu**[1,2], **Brandon Nakashima**[1], **Sunju Lee**[1,2], **Young Jin Seong**[1,2], **Wan Jiao**[1], **Chester J. Koh**[3], **Peter Baluk**[4], **Donald M. McDonald**[4], **Sindhu Saraswathy**[5], **Jong Y. Lee**[5], **Noo Li Jeon**[6], **Zhenqian Zhang**[7], **Alex S. Huang**[5], **Bin Zhou**[7], **Alex K. Wong**[8], **Young-Kwon Hong**[1,2]

[1]Department of Surgery, Norris Comprehensive Cancer Center, Keck School of Medicine, University of Southern California, Los Angeles, California, USA

[2]Department of Biochemistry and Molecular Medicine, Norris Comprehensive Cancer Center, Keck School of Medicine, University of Southern California, Los Angeles, California, USA

[3]Division of Pediatric Urology, Texas Children's Hospital, Baylor College of Medicine, Houston, Texas, USA

[4]Cardiovascular Research Institute, UCSF Helen Diller Family Comprehensive Cancer Center, and Department of Anatomy, University of California, San Francisco, San Francisco, California, USA

[5]Doheny Eye Institute and Department of Ophthalmology, David Geffen School of Medicine at UCLA, Los Angeles, California, USA

[6]Department of Mechanical and Aerospace Engineering, Seoul National University, Seoul, Republic of Korea

[7]State Key Laboratory of Cell Biology, Shanghai Institute of Biochemistry and Cell Biology, Center for Excellence in Molecular Cell Science, University of Chinese Academy of Sciences, Chinese Academy of Sciences, Shanghai, China

[8]Division of Plastic Surgery, City of Hope National Medical Center, Duarte, California, USA.

Abstract

Correspondence should be addressed to: Young-Kwon Hong, Ph.D., Department of Surgery, Keck School of Medicine, University of Southern California, Los Angeles, CA 90033, Tel: 323-442-7825, young.hong@usc.edu.

Disclosures

Alex S. Huang discloses his relationships with Santen Pharmaceutical (Consultant), Allergan (Consultant), Aerie Pharmaceuticals (Consultant), Heidelberg Engineering (Research Support), Glaukos Corporation (Research Support), and Diagnosys (Research Support). All other authors disclose no conflict of interest with this study.

Supplemental Material

Supplemental Expanded Materials and Methods

Figures S1 – S8

References 68–69

Background: Mutations in *PIEZO1* cause human lymphatic malformations. We have previously uncovered an Orai1-mediated mechanotransduction pathway that triggers lymphatic sprouting through Notch downregulation in response to fluid flow. However, the identify of its upstream mechanosensor remains unknown. This study aimed to identify and characterize the molecular sensor that translates the flow-mediated external signal to the Orai1-regulated lymphatic expansion.

Methods: Various mutant mouse models, cellular, biochemical, and molecular biology tools, and a mouse tail lymphedema model were employed to elucidate the role of Piezo1 in flow-induced lymphatic growth and regeneration.

Results: Piezo1 was found to be abundantly expressed in lymphatic endothelial cells (LECs). Piezo1 knockdown in cultured LECs inhibited the laminar flow-induced calcium influx and abrogated the flow-mediated regulation of the Orai1 downstream genes, such as Klf2, Dtx1, Dtx3L, and Notch1, which are involved in lymphatic sprouting. Conversely, stimulation of Piezo1 activated the Orai1-regulated mechanotransduction in the absence of fluid flow. Piezo1-mediated mechanotransduction was significantly blocked by Orai1 inhibition, establishing the epistatic relationship between Piezo1 and Orai1. Lymphatic-specific conditional Piezo1 knockout largely phenocopied sprouting defects shown in Orai1- or Klf2- knockout lymphatics during embryo development. Postnatal deletion of Piezo1 induced lymphatic regression in adults. Ectopic Dtx3L expression rescued the lymphatic defects caused by Piezo1 knockout, affirming that the Piezo1 promotes lymphatic sprouting through Notch downregulation. Consistently, transgenic Piezo1 expression or pharmacological Piezo1 activation enhanced lymphatic sprouting. Finally, we assessed a potential therapeutic value of Piezo1 activation in lymphatic regeneration and found that a Piezo1 agonist, Yoda1, effectively suppressed post-surgical lymphedema development.

Conclusions: Piezo1 is an upstream mechanosensor for the lymphatic mechanotransduction pathway and regulates lymphatic growth in response to external physical stimuli. Piezo1 activation presents a novel therapeutic opportunity for preventing post-surgical lymphedema. The Piezo1-regulated lymphangiogenesis mechanism offers a molecular basis for Piezo1-associated lymphatic malformation in humans.

Graphical Abstract

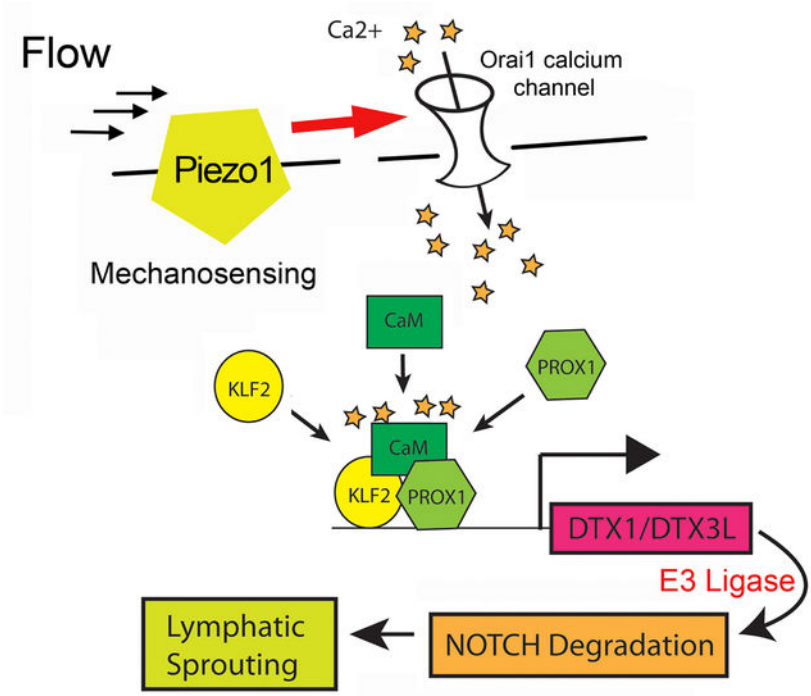

Keywords

Vascular biology

INTRODUCTION

The lymphatic system controls tissue fluid homeostasis, immune cell trafficking, and dietary lipid absorption [1]. It consists of lymphatic vascular networks and secondary lymphoid organs. The initial lymphatics begin from the interstitial space in the tissues, where fluid, molecules, and cells are drained into the lymphatic vessel lumen through lymphatic endothelial cell (LEC) junctions. These initial lymphatics connect to thicker lymphatic collectors that are invested with lymphatic muscle cells and also equipped with luminal valves [2]. During embryonic development, LECs are continually exposed to unidirectional laminar flow to cope with the growing amount of tissue fluid. Similarly, lymphatics under pathological conditions experience significant fluid flow due to increased lymph flow. These fluid flows are known to trigger lymphatic sprouting and expansion through activation of mechanotransduction mechanisms [3–5]. Organ-specific lymphatic functionality and morphology have been shown to be directly associated with the lymphatic flow [6–8].

Mechanotransduction plays an essential role in the development, maintenance, and function of the cardiovascular system [9, 10]. It is believed that fluid flow is a critical non-biological signal that promotes lymphatic sprouting, growth, and valve formation. Since fluid drainage is the lymphatic system's primary function, flow-triggered activation of lymphatic expansion has offered a conceptual paradigm for mechanotransduction pathways in lymphatics. This idea parallels with the genetic programs governing hypoxia-driven angiogenesis. Studies

have shown that fluid flow activates LEC proliferation and migration, VEGF-C expression, and lymphatic network formation. Embryonic lymphatic development coincides with increased embryonic fluid drainage [3]. Collecting lymphatic vessel maturation and luminal valve development are regulated by lymph drainage and flow *in vivo* [3]. Moreover, interstitial flow could enhance lymphatic sprouting and synergize with traditional biological factors to promote lymphatic growth [3]. Therefore, flow-mediated mechanical stimulation is a critical expansion signal for the lymphatic system.

Piezo1 is a mechanically activated cation channel and functions as a mechano-transducer that senses different types of external forces [11, 12]. Piezo1 has attracted tremendous attention owing to its unique protein structure. It forms an ion channel of a homotrimeric propeller-like structure with a central cap domain and the extracellular domains resembling three blades composed of 38 transmembrane helical units. These extracellular blade domains are connected to the central intracellular domain through three long beam-like structures that enable a mechanogating mechanism [11, 12]. Yoda1, a small molecule Piezo1 agonist, was identified as an active compound that delays the inactivation kinetics of mechanically-activated responses of Piezo1 [13]. Yoda1 specifically binds to a pocket located in the putative mechanosensory domain of Piezo1 and, acting as a molecular wedge, lowers the channel's mechanical threshold for activation [14]. In the absence of membrane tension, Yoda1 acts like a wedge by decoupling these two domains, increasing tension-induced arm extension [14]. This wedge-like effect extends the channel opening status even by sub-threshold stimuli [14]. Importantly, Yoda1 does not display significant toxicities *in vitro* and in animals [15–22]. EC_{50} of Yoda1 was initially estimated at 10–20 μM based on studies using Piezo1-overexpressing HEK293 cells [13]. However, Yoda1 was still effective on primary endothelial cells at concentrations ranging from 0.12 – 1.0 μM [22–24]. One explanation for this discrepancy could be that primary endothelial cells may be uniquely sensitive to Yoda1. Therefore, the molecular basis of this unexpected sensitivity warrants further investigations.

Piezo1 regulates various aspects of vascular development, function, and maintenance by controlling fluid flow-induced mechanotransduction pathways [25, 26]. In particular, Piezo1 regulates endothelial cell shape and vascular architecture in response to physiological force [12, 25]. It controls blood pressure by mediating flow-induced ATP release [23] and acts as a sensor for whole-body physical activities such as exercise [27]. Piezo1 has also been reported to play a critical role in the lymphatic system. We and others have recently reported that Piezo1 is required for lymphatic valve formation by incorporating mechanical force signals into the valve-forming genetic program [22, 28]. Importantly, human genetic studies have identified Piezo1 mutations as responsible for generalized lymphatic dysplasia (GLD) [29, 30].

We have recently elucidated molecular mechanisms underlying the flow-induced expansion of the lymphatics [4, 5, 22]. We reported that unidirectional flow activates calcium influx through Orai1 and triggers proliferation of LECs, but not blood vascular endothelial cells (BECs) [4]. We elucidated a lymphatic-specific mechanism responsible for flow-induced Notch downregulation and sprouting lymphangiogenesis [5]. However, the mechanosensor that senses the flow-induced mechanical force remains unknown. In this study, we aimed to identify and characterize the molecular sensor that triggers the LEC-specific mechanotransduction pathway. Together, we defined the role of Piezo1 in lymphatic

expansion by elucidating the molecular and functional relationship between Piezo1 and Orai1 and also extended the experimental outcome toward developing Piezo1 activation as a novel therapeutic approach to preventing post-surgical lymphedema.

METHODS

Data Availability.

Detailed materials and methods are available in the Supplemental Methods and Supplemental Major Resources Table. The authors declare that all supporting data are available within the article and its online supplementary files.

RESULTS

Piezo1 Is Required for Flow-Induced Notch Downregulation in Lymphatic Endothelial Cells

Our previous reports [4, 5] proposed a lymphatic-specific mechanotransduction model, which translates the fluid flow-induced shear stress signal to Notch downregulation and lymphatic sprouting (Figure S1). In this model, mechanosensor(s) senses the flow-induced force and activates the Orai1 calcium channel, promoting intracellular calcium entry. Calcium-loaded calmodulin (CaM) binds to Prox1 and Klf2 proteins, forming a transcription factor complex that occupies the promoters of *DTX1* and *DTX3L* and upregulates their gene expressions. Dtx1 and Dtx3L function as Notch E3 ligases and downregulate Notch activity, hence promoting lymphatic sprouting. However, it is unknown which mechanosensor(s) senses fluid force and activates Orai1-mediated calcium entry. In this study, we aimed to identify the mechanosensor that acts upstream of Orai1 in LECs. Because Piezo1 has been associated with GLD [29, 30], we investigated Piezo1 among other known mechanosensing proteins [31] for its involvement in the Orai1-mediated mechanotransduction. A recent single-cell RNA sequencing study has reported the expression of Peizo1 in adult mouse mesenteric lymphatics [32]. However, Piezo1 expression in developing embryonic dermal lymphatics remains to be studied. Thus, we first evaluated the expression of Piezo1 in human dermal LECs and BECs and found that Piezo1 and Orai1 are comparably expressed in both cell types (Figure 1A, Figure S2A). Moreover, Piezo1 expression was further verified in endothelial cells of developing embryos (E14.5 and E15.5) using a new reporter mouse line showing the endogenous expression of Piezo1 *in vivo* (Figure 1B). This new reporter mouse was prepared by crossing a novel Piezo1-CreER^{T2}-BFP driver line [33] with Ai47 Cre-reporter line (CAG-LoxP-STOP-LoxP-3X GFP) [34]. Piezo1-CreER^{T2}-BFP driver line was created by inserting a DNA cassette harboring the CreER^{T2}-P2A-BFP-WPRE-polyA signal immediately after the ATG start codon of Piezo1 [33]. Thus, Tamoxifen-responsive Cre (CreER^{T2}) is produced in all cells expressing Piezo1 and, when crossed with a reporter line (Ai47-RCL-TriGFP), will mark Piezo1-expressing cells [33]. This innovative mouse model enabled us to demonstrate abundant expression of Piezo1 in endothelial cells of embryonic back skins. We then evaluated the role of Piezo1 in intracellular calcium influx in LECs in response to fluid flow by siRNA-mediated knockdown. Like Orai1 knockdown [5], Piezo1 knockdown significantly inhibited flow-activated calcium entry in LECs and flow-induced Notch1 downregulation (Figure 1C–E, Figure S2B and S2C). In addition, Piezo1 knockdown significantly reduced the flow-mediated regulation of Dtx1, Dtx3L, Klf2, and

Notch1 (Figure 1F, Figure S2D). Together, these data suggest that Piezo1 is necessary for flow-induced downregulation of the Notch signal.

Piezo1 Functions as a Mechanosensor Upstream of Orai1 in Lymphatic Endothelial Cells

Conversely, we next asked whether Piezo1 overexpression is sufficient to activate the Orai1-controlled mechanotransduction in the absence of fluid flow. Indeed, Piezo1 overexpression alone could recapitulate the flow-mediated regulation of Orai1 downstream genes, such as upregulation of Dtx1, Dtx3L, and Klf2 and downregulation of Notch1 intracellular domain (NICD1) (Figure 2A, Figure S3A). Consistent with these results, treatment of a Piezo1 agonist Yoda1 [13] induced these flow phenotypes in LECs in the absence of flow (Figure 2B, Figure S3B), and these Yoda1-induced phenotypes were mediated through Piezo1 (Figure 2C, Figure S3C). To determine the epistatic relationship between Piezo1 and Orai1, we overexpressed Piezo1 first and then inhibited Orai1 using a chemical inhibitor (SKF-96365). Notably, Orai1 inhibition significantly, although not completely, blocked the Piezo1-induced NICD1 downregulation (Figure 2D, Figure S3D). These data suggest that Piezo1-induced NICD1 downregulation is substantially mediated by Orai1 and also by some other unknown mechanisms. Consistently, Yoda1 treatment increased the calcium concentration, and this intracellular calcium influx was significantly but entirely reduced by Orai1 inhibition (Figure 2E). Finally, we asked whether Orai1 activation alone recapitulates the flow-induced gene regulation in LECs. For this purpose, we employed a new selective pharmacological enhancer of the Orai1 (IA65) [35], which has recently been developed and shown to enhance Orai1-mediated Calcium influx without the cytotoxicity caused by sustained Orai1 activation. Indeed, Orai1 stimulation with IA65 resulted in upregulation of Dtx1 and Dtx3L and downregulation of Notch in the absence of flow (Figure 2F, Figure S3E). This phenotype was largely abolished following Orai1 knockdown, but not Piezo1 knockdown (Figure 2G, Figure S3F), suggesting that Orai1 mediates the IA65 effects and that Piezo1 acts upstream of Orai1. Thus, Orai1 stimulation alone was sufficient for the LEC mechanotransduction without fluid flow or Piezo1 activation. Together, these studies demonstrate that Piezo1 is an upstream activator of Orai1 in the laminar flow-activated mechanotransduction pathway in LECs.

Piezo1 KO Resembles Lymphatic Sprouting Defects in Orai1 KO, Klf2 KO, and Notch1 TG Embryos.

We next characterized the lymphatic sprouting phenotypes in embryos after lymphatic-specific inducible loss-of-function of Piezo1, Orai1, and Klf2. Pregnant female mice from crossing *Prox1-CreER*^{T2} mice [36] with Piezo1 [37], Orai1 [4, 5], or Klf2 [38] floxed mice were injected with Tamoxifen at E11.5 and 13.5. Embryo back skins were harvested at E15.5 for whole-mount staining to visualize the lymphatics (Figure 3A). Efficient Cre-mediated gene excision was confirmed by genotyping of target tissues (Figure S4). While the control embryos showed sprouting lymphatic vessels with jagged-shaped tip cells, Piezo1-deficient lymphatics in *Prox1-CreER*^{T2}; *Pieoz1* $^{fl/fl}$ (hereafter Piezo1$^{\Delta LEC}$) embryos displayed round-ended lymphatic vessels without new sprouts (Figure 3B–E). Importantly, these sprouting defects of Piezo1-deficient lymphatics resemble those shown in Orai1-null lymphatics or Klf2-null lymphatics of the embryos of *Prox1-CreER*^{T2}; *Orai1* $^{fl/fl}$ and *Prox1-CreER*^{T2}; *Klf2* $^{fl/fl}$, respectively (Figure 3F–M) [5]. In addition, because our hypothesis expects that

deletion of Piezo1, Orai1, or Klf2 would commonly lead to upregulation of Notch activity in LECs (Figure S1), we also examined the phenotypes of lymphatic-specific inducible Notch1 gain-of-function mice ($NICD1^{TG}$) [39]. Indeed, ectopic activation of the Notch1 pathway generated round-ended lymphatic vessels without new sprouts (Figure 3N–Q), resembling the defective lymphatic sprouting phenotypes shown in Piezo1-, Orai1-, or Klf2-deficient lymphatics. Therefore, these four lymphatic-specific conditional mutant embryos commonly demonstrated significantly reduced numbers of lymphatic sprouts and branch points as well as increased vessel thickness compared to wild-type embryos (Figure 3R–T). These data demonstrate the essential role of Piezo1 in sprouting lymphangiogenesis, consistently supporting our hypothesis that Piezo1, Orai1, Klf2, and Notch1 constitute an essential mechanotransduction pathway that controls lymphatic sprouting in response to fluid flow.

Essential Role of Piezo1 in Postnatal Lymphatic Maintenance

We next investigated the role of Piezo1 in lymphatic maintenance. A lymphatic reporter transgene (*Prox1-tdTomato*) [40] was introduced to *Prox1-CreER^{T2}*; *Pieoz1 $^{fl/fl}$* mice by genetic crossings to directly visualize lymphatic vessels (Figure 4A). Lymphatic-specific deletion of Piezo1 was induced in 3-week-old postnatal mice and evaluated its impact at 7-week. Notably, lymphatic-specific Piezo1 deletion caused significant lymphatic regression in the mesentery and hindlimb, as evidenced by reduced branch point numbers per vessel length and increased distance between two branch points in both vascular beds (Figure 4B–M). Together, these studies demonstrate an essential role of Piezo1 in the postnatal maintenance of lymphatic vessels.

Dtx3L Overexpression Rescues the Piezo1-Null Lymphatic Phenotypes

Our hypothesis proposes that the flow-induced Notch downregulation is caused by Dtx1 and/or Dtx3L, that act as Notch E3 ligases (Figure S1). We thus asked whether the lymphatic phenotypes in Piezo1 KO could be rescued by ectopic overexpression of Dtx1 and/or Dtx3L. For this, we crossed an inducible Dtx3L transgenic line (TG) [5] with mice harboring *Prox1-tdTomato, Prox1-CreER^{T2}*, and/or *Piezo1 $^{fl/fl}$* alleles and harvested embryos that allow Piezo1 deletion and/or Dtx3L ectopic expression, individually or simultaneously, in LEC-specific manner (Figure 5A). Notably, Dtx3L ectopic expression increased lymphatic sprouting based on lymphatic vessel tip number, branching points number, and distance between two branching points (Figure 5B–E, J–M). More importantly, when Piezo1 deletion and Dtx3L overexpression were simultaneously achieved, the lymphatic defects caused by Piezo1 deletion were entirely rescued by Dtx3L ectopic expression (Figure 5B–M). These studies consistently support our hypothesis that Piezo1 triggers lymphatic expansion during development through activation of the Orai1-mediated mechanotransduction.

Piezo1 Overexpression Is Sufficient to Promote Lymphatic Sprouting

We next asked whether enhancing Piezo1 activity (gain-of-function) in lymphatics would promote lymphatic expansion during embryonic and postnatal development. A fraction of the Piezo1 channel is known to spontaneously open in the absence of force [41]. Consistently, Yoda1, which primarily affects the inactivation kinetics of Piezo1, could increase Piezo1-mediated calcium influx in the absence of pressure [13]. These studies

suggest that increased expression of Piezo1 protein would sensitize the cells to the flow-induced mechanotransduction. Therefore, we generated a conditional transgenic mouse line (Piezo1^{TG}) capable of ectopic expression of mouse Piezo1 upon Tamoxifen administration (Figure 6A). This Piezo1^{TG} allele consists of a constitutive promoter (CAG), LoxP site, EGFP, 4-tandem copies of poly-A, LoxP site, and mouse Piezo1 cDNA. The CAG promoter encodes EGFP only until the Cre recombinase excises the EGFP-4X pA fragment out, which leads to the expression of Piezo1 cDNA. This line was crossed with *Prox1-CreER^{T2}; Prox1-tdTomato* line, and pregnant females were injected with Tamoxifen to induce lymphatic-specific Piezo1 expression. Piezo1 overexpression was confirmed on lymph node-derived LECs using immunofluorescence assays and western blot analyses (Figure S5). Indeed, ectopic Piezo1 overexpression significantly enhanced sprouting lymphangiogenesis (Figure 6B, C). Moreover, induction of Piezo1 overexpression in newborns (P0) promoted mesenteric lymphatic sprouting and network formation (Figure 6D, E). These data suggest that ectopic Piezo1 expression is sufficient to enhance lymphatic expansion and network formation.

Yoda1 Activates Lymphatic Expansion in the Skin and Eye

We next evaluated the pro-lymphangiogenic effects of a molecular or chemical stimulation of Piezo1. When overexpressed, both human and mouse Piezo1 enhanced the proliferation of LECs (Figure 7A). Yoda1 treatment significantly stimulated LEC proliferation at sub-micromolar concentrations (Figure 7B). When expression of Orai1 or Piezo1 was inhibited by siRNA-mediated knockdown, Yoda1 did not promote LEC proliferation (Figure 7C). Using an organ-on-a-chip platform [42], we tested the effect of Yoda1 on 3-D lymphatic vessel formation. Yoda1 treatment increased vessel density, thickness, vascular tips, and branch points compared to vehicle (Figure 7D, E), indicating a potent pro-lymphangiogenic effect of Yoda1. Consistent with this notion, Yoda1 treatment immediately activated ERK1/2 phosphorylation in LECs within 15 minutes (Figure 7F). Furthermore, Orai1 activation using IA65 also significantly promoted 3-D lymphatic network formation (Figure S6). We then assessed *in vivo* lymphangiogenic efficacy of Yoda1 by conducting the following three lines of animal-based assays. First, we intraperitoneally (i.p.) injected Prox1-EGFP lymphatic reporter mice [43] with Yoda1 or vehicle daily for 35 days and examined dermal lymphatic vasculatures in the ears. Indeed, Yoda1 activated lymphatic sprouting and lymphatic valve formation (Figure 7G, H). We next took advantage of the conjunctival lymphatic networks in adult eyes. As we recently reported [44, 45], the conjunctival lymphatic network progressively develops from the nasal side and maintains this polarized distribution in adults. We injected Yoda1 or vehicle into the subconjunctival area of Prox1-tdTomato reporter mice [40]. After seven days, we detected significant expansion of the conjunctival lymphatics in Yoda1-injected eyes but not in vehicle-injected eyes (Figure 7I, J). In comparison, Yoda1 did not induce statistically significant lymphatic expansion in the trachea of adult mice (Figure S7). Lastly, we conducted a Matrigel implant assay. Matrigel pre-mixed with Yoda1 or vehicle was subcutaneously injected into Prox1-EGFP reporter mice. After two weeks, the Matrigel plugs were harvested and analyzed for lymphatic ingrowth. Indeed, Yoda1 activated lymphatic invasion into the Matrigel implants (Figure 7K, L). Together, our studies suggest that Yoda1 is a pro-lymphangiogenic agent and can activate lymphatic expansion in animal models.

Therapeutic Efficacy of Yoda1 in A Mouse Lymphedema Model

We evaluated the potential therapeutic efficacy of Yoda1 on surgery-associated lymphedema. Mousetail lymphedema is a widely accepted animal model that mimics the pathophysiology of human lymphedema [46–48]. Prox1-EGFP adult mice were subjected to tail lymphedema surgery, and subsequently, i.p. injected with vehicle or Yoda1 at two different dosages: low dose (71 μg/kg/day) and high dose (213 μg/kg/day), which were extrapolated from our cell culture-based studies. We confirmed the immediate effect of Yoda1 treatment by increased ERK1/2 phosphorylation in lymph node-derived LECs (Figure S8). Daily Yoda1 administration for 35 days showed a notable therapeutic efficacy in ameliorating the surgery-induced tail swelling (Figure 8A, B). Yoda1 treatment at these dosages did not cause any significant toxicities or mortalities during this period, determined by complete blood count (CBC) and comprehensive metabolic panel (CMP) (data not shown). In addition, we performed tail lymphangiography as a functional test by injecting a fluorescent dye Indocyanine Green (ICG) into the tail tips and measuring the remaining ICG amount over four days. This study revealed that the Yoda1-treated groups cleared ICG tracer at a significantly faster rate than the vehicle-treated group (Figure 8C, D), indicating that reduced tail swelling was attributable to improved fluid drainage by Yoda1. Histological analyses of tail cross-sections confirmed that Yoda1 treatment largely prevented cutaneous edema formation and collagen deposition that were prominently detectable in the vehicle-treated mice (Figure 8F, G). Finally, Lyve1 staining revealed increased lymphatic vessel number and size in Yoda1-treated groups than in the control group (Figure 8H, I). Together, our studies uncovered a potential therapeutic efficacy of Yoda1 in preventing surgery-associated lymphedema formation.

DISCUSSION

The primary role of the lymphatic system is proper regulation of tissue fluid drainage. Consistent with this notion, fluid accumulation in the tissue triggers lymphatic expansion to increase lymphatic drainage capacity. It has been postulated that increased luminal flow, consequential to fluid accumulation, could generate a critical non-biological signal that activates lymphatic sprouting and growth [3, 9]. The concept of fluid flow-induced lymphatic growth parallels the established causal relationship between tissue hypoxia and angiogenesis. Nonetheless, compared to the well-established mechanism underlying the hypoxia-driven angiogenesis, the molecular basis for the fluid flow-induced lymphatic expansion has not been fully defined.

The current work extends our previous study of the lymphatic-specific mechanism underlying the flow-induced sprouting lymphangiogenesis [5]. In the previously proposed mechanism (Figure S1), fluid flow activates Orai1, an essential subunit of the calcium release-activated calcium channel (CRAC) [49, 50], and increases the intracellular calcium influx. Subsequently, calcium-loaded calmodulin forms a protein complex with Klf2 (known as a master regulator of shear stress responses) [51] and Prox1 (functioning as the master regulator of lymphatic development) [52]. This protein complex then binds to the promoters of Dtx1 and Dtx3L and activates their gene expression. In turn, Dtx1 and Dtx3L proteins form a Notch E3 ligase complex [53], which decreases Notch activity and promotes lymphatic

sprouting. We proposed that this mechanotransduction pathway translates the external fluid force to a biological signal that activates lymphatic expansion. Notably, this mechanism seems to operate only in lymphatics where Prox1 is expressed. We found that Orai1 deletion in blood vessels or Orai1 knockdown in cultured blood vessel endothelial cells (BECs) displayed the opposite or no effects [5]. Previous studies have consistently demonstrated that fluid flow increased Notch activity in blood vessels [54–57]. We attributed the lymphatic specificity of this mechanism to the lymphatic-specific upregulation of Dtx3L in response to fluid flow [5], as well as the lymphatic-specific expression of Prox1, a master regulator of lymphatic development [52]. Despite this, the identity of the molecular sensors that sense the external fluid force and trigger the Orai1-mediated calcium influx in LECs remained unknown. This study identified Piezo1 as a mechanosensor that activates lymphatic expansion in response to fluid flow.

Several mechanosensing molecules have been associated with endothelial mechanotransduction, including Piezo1/2, integrins, PECAM1, VEGFR2, and VE-Cadherin [3]. Among them, as mutations in Piezo1 have been reported to cause an autosomal recessive generalized lymphatic dysplasia [29, 30], we chose to investigate Piezo1 as the top candidate molecule that may function upstream of Orai1. We present data that identify Piezo1 as an upstream mechanosensor of the Orai1-mediated mechanotransduction pathway in LECs. Our loss-of-function studies using lymphatic Piezo1 KO mice revealed the essential role of Piezo1 in embryonic development and postnatal maintenance of the lymphatics. In addition, the gain-of-function studies using novel Piezo1 transgenic mice and a chemical agonist, Yoda1, demonstrated the sufficiency of Piezo1 in inducing lymphatic expansion in embryos and adults. These findings led us to ask whether activation of Piezo1 would enhance lymphangiogenesis and prevent surgery-associated lymphedema formation using a mouse lymphedema model. Indeed, Yoda1 was found to effectively prevent tissue swelling and associated fibrosis through enhanced lymphatic growth, indicating a therapeutic potency of Yoda1 against surgery-associated lymphedemas.

Importantly, mutations in *PIEZO1* have been associated with autosomal recessive GLD [29, 30]. GLD is a congenital lymphedema characterized by widespread lymphedema throughout the body, such as facial dysmorphism and limb edema, and systemic involvement, including intestinal and pulmonary lymphangiectasia, pleural and pericardial effusion, and chylothorax [30]. An autosomal recessive GLD has previously been reported in Hennekam Lymphangiectasia-Lymphoedema syndrome, caused by mutations in *CCBE1* [58] and *FAT4* [59]. Along with these two genes, *PIEZO1* is the third gene for GLD [30]. The fact that *PIEZO1* mutations cause GLD in humans offers robust support to our current study defining the role of Piezo1 in lymphatic development and maintenance in mice. Our study revealed that Piezo1 deletion in embryonic lymphatics caused widespread lymphatic malformation during development characterized by sprouting defects, less branching, and delayed valve formation. Moreover, Piezo1 deletion in postnatal or adult lymphatics resulted in significant lymphatic vessel regression.

Our finding of the Piezo1-mediated activation Orai1 calcium channel raises another important question how activation of one calcium channel (Piezo1) leads to activation of another calcium channel (Orai1). Notably, this kind of Piezo1 functional mode has

already been reported by previous studies [23, 60, 61]; only a minor fraction of the increased cytoplasmic calcium is attributable to Piezo1-mediated calcium influx, and the majority of the elevated calcium amount by Piezo1 activation is due to some other downstream amplification mechanisms. For example, Piezo1 plays an essential role in mechanotransduction in BECs, where blocking of G_q/G_{11} proteins suppresses the large fraction of Piezo1-induced calcium entry, suggesting other downstream amplification mechanisms accounting for most of the increased calcium [62]. Nonetheless, the precise mechanism for the Piezo1-mediated Orai1 activation in LECs is yet to be defined. Both Piezo1 and Orai1 are membrane-bound calcium channels capable of extracellular calcium uptake. One possibility is that Piezo1 physically interacts with Orai1 and actives its calcium uptake. Binding proteins of Piezo1 have recently been identified, including sarcoplasmic/endoplasmic-reticulum Ca^{2+} ATPases (SERCA) [63]. SERCA2 binds to an intracellular linker of Piezo1 that connects the pore-module and mechanotransduction-module and subsequently suppresses its calcium channeling function [63]. Because Orai1 is a well-known CRAC that triggers the store-operated calcium entry (SOCE) channel, it would be exciting to investigate the potential physical interaction between Piezo1 and Orai1. Another functional scenario is that Piezo1, like many cytokines/chemokines receptors, may activate the Orai1-mediated calcium entry by inducing ER calcium release through direct stimulation of the ER calcium channels such as IP_3 receptors and ryanodine receptors [64]. The third scenario is that Piezo1 may also be present in the ER membrane and function as an ER calcium channel that directly exports calcium from the ER. Previous studies reported the presence of Piezo1 not only in the cytoplasmic membrane but also in other intracellular membranes, including ER membranes [65–67]. It is thus possible to speculate that Piezo1 present in the ER membrane could sense the external mechanical force and consequently export calcium from the ER to the cytoplasm. If so, Stromal Interaction Molecule (STIM) proteins would detect this ER calcium depletion and immediately activate Orai1 [64]. We favor this mechanism, but it is not mutually exclusive to the second scenario as the cytoplasmic membrane-bound Piezo1 would still activate other ER membrane-bound channels via cAMP and other intermediate molecules. Therefore, a further in-depth investigation will be needed to address this exciting question.

Because of its unique biochemical, molecular, and functional characteristics with clearly visible clinical values, Piezo1 has been an attractive therapeutic target for various human diseases. Thus, significant efforts have been spent to identify its agonists. Most notably, Yoda1 was identified as the first Piezo1 chemical agonist after screening ~3.25 million compounds using a cell-based fluorescence assay [13]. Yoda1 was found to bind to a putative mechanosensory domain and, acting as a molecular wedge, facilitate the force-induced conformational changes, thus lowering the channel's mechanical threshold for activation [14]. Nonetheless, Yoda1 has been considered an undesirable drug candidate due to its low solubility and high EC_{50} (10–20 μM) determined by electrophysiological assays (calcium current) using Piezo1-overexpressing HEK293 cells [13]. However, Yoda1 could effectively induce various cellular and molecular phenotypes in human primary endothelial cells even at a concentration of 0.12–1.0 μM [22–24], approximately 50–100 times lower than the initially reported EC_{50} [13]. Although different assays were employed to estimate the EC_{50} values, it is possible that endothelial cells may be uniquely sensitive to Yoda1. Based on this *in vitro*

concentration data, we determined effective *in vivo* dosages of Yoda1 using fluid drainage assays and chose low (71 μg/kg/day) and high (213 μg/kg/day) dosages for the current studies. We did not note any Yoda1 solubility problems at these dosages. More importantly, mice continuously treated with Yoda1 at these dosages for 35 days did not develop any significant health issues or notable changes in their blood biochemistry (data not shown). Considering that Piezo1 is expressed in various cell types and that Piezo1 loss-of-function mutations have been associated with human diseases, Yoda1 or its further optimized analogs could be drug candidates. Therefore, the potential therapeutic values of Piezo1 agonists are worthy of further investigation.

In conclusion, our study defined a molecular mechanism underlying flow-induced lymphatic expansion. In particular, we identified Piezo1 as a mechanosensor that senses the flow-generated mechanical force and triggers Orai1-induced calcium influx. Accordingly, our studies revealed a pro-lymphangiogenic property of Piezo1 activation. A Piezo1 agonist, Yoda1, was found to be capable of activating lymphatic expansion in a mouse lymphedema model, suggesting its potential therapeutic value against post-surgical lymphedema. Moreover, the newly defined Piezo1-controlled mechanotransduction pathway provides a molecular basis for the generalized lymphatic dysplasia caused by *PIEZO1* mutations in humans. Overall, the outcome of our work offers a better understanding of how the lymphatics expand in response to increased tissue fluid volume and flow.

Supplementary Material

Refer to Web version on PubMed Central for supplementary material.

Sources of Funding

This study was supported by the National Institutes of Health (HL141857, CA250065, DK114645 to YKH; EY030501 to ASH; HL132110 to AKW; HL127402, HL059157, HL143896 to DMcD), American Cancer Center (#IRG-16-181-57 to DC), the Glaucoma Research Foundation (Shaffer Grant to ASH), and the Leducq Foundation (11CVD03 to DMcD).

Non-standard Abbreviations and Acronyms

LEC	lymphatic endothelial cell
GLD	generalized lymphatic dysplasia
BEC	blood vascular endothelial cell
CaM	calmodulin
CreER^{T2}	Cre recombinase (Cre) fused to a mutant estrogen ligand-binding domain
Piezo1$^{\Delta LEC}$	Piezo1 deletion in lymphatic endothelial cells
NICD1	Notch1 intracellular domain

REFERENCES

1. Escobedo N and Oliver G. Lymphangiogenesis: Origin, Specification, and Cell Fate Determination. Annu Rev Cell Dev Biol. 2016;32:677–691. [PubMed: 27298093]
2. Breslin JW, Yang Y, Scallan JP, Sweat RS, Adderley SP and Murfee WL. Lymphatic Vessel Network Structure and Physiology. Compr Physiol. 2018;9:207–299. [PubMed: 30549020]
3. Geng X, Ho YC and Srinivasan RS. Biochemical and mechanical signals in the lymphatic vasculature. Cell Mol Life Sci. 2021.
4. Choi D, Park E, Jung E, Seong YJ, Hong M, Lee S, Burford J, Gyarmati G, Peti-Peterdi J, Srikanth S, Gwack Y, Koh CJ, Boriushkin E, Hamik A, Wong AK and Hong YK. ORAI1 Activates Proliferation of Lymphatic Endothelial Cells in Response to Laminar Flow Through Kruppel-Like Factors 2 and 4. Circ Res. 2017;120:1426–1439. [PubMed: 28167653]
5. Choi D, Park E, Jung E, Seong YJ, Yoo J, Lee E, Hong M, Lee S, Ishida H, Burford J, Peti-Peterdi J, Adams RH, Srikanth S, Gwack Y, Chen CS, Vogel HJ, Koh CJ, Wong AK and Hong YK. Laminar flow downregulates Notch activity to promote lymphatic sprouting. J Clin Invest. 2017;127:1225–1240. [PubMed: 28263185]
6. Ahn JH, Cho H, Kim JH, Kim SH, Ham JS, Park I, Suh SH, Hong SP, Song JH, Hong YK, Jeong Y, Park SH and Koh GY. Meningeal lymphatic vessels at the skull base drain cerebrospinal fluid. Nature. 2019;572:62–66. [PubMed: 31341278]
7. Petrova TV and Koh GY. Organ-specific lymphatic vasculature: From development to pathophysiology. J Exp Med. 2018;215:35–49. [PubMed: 29242199]
8. Petrova TV and Koh GY. Biological functions of lymphatic vessels. Science. 2020;369.
9. Urner S, Kelly-Goss M, Peirce SM and Lammert E. Mechanotransduction in Blood and Lymphatic Vascular Development and Disease. Adv Pharmacol. 2018;81:155–208. [PubMed: 29310798]
10. Swartz MA and Boardman KC Jr. The role of interstitial stress in lymphatic function and lymphangiogenesis. Ann N Y Acad Sci. 2002;979:197–210; discussion 229–34. [PubMed: 12543729]
11. Coste B, Xiao B, Santos JS, Syeda R, Grandl J, Spencer KS, Kim SE, Schmidt M, Mathur J, Dubin AE, Montal M and Patapoutian A. Piezo proteins are pore-forming subunits of mechanically activated channels. Nature. 2012;483:176–81. [PubMed: 22343900]
12. Li J, Hou B, Tumova S, Muraki K, Bruns A, Ludlow MJ, Sedo A, Hyman AJ, McKeown L, Young RS, Yuldasheva NY, Majeed Y, Wilson LA, Rode B, Bailey MA, Kim HR, Fu Z, Carter DA, Bilton J, Imrie H, Ajuh P, Dear TN, Cubbon RM, Kearney MT, Prasad KR, Evans PC, Ainscough JF and Beech DJ. Piezo1 integration of vascular architecture with physiological force. Nature. 2014;515:279–82. [PubMed: 25119035]
13. Syeda R, Xu J, Dubin AE, Coste B, Mathur J, Huynh T, Matzen J, Lao J, Tully DC, Engels IH, Petrassi HM, Schumacher AM, Montal M, Bandell M and Patapoutian A. Chemical activation of the mechanotransduction channel Piezo1. Elife. 2015;4.
14. Botello-Smith WM, Jiang W, Zhang H, Ozkan AD, Lin YC, Pham CN, Lacroix JJ and Luo Y. A mechanism for the activation of the mechanosensitive Piezo1 channel by the small molecule Yoda1. Nat Commun. 2019;10:4503. [PubMed: 31582801]
15. Evans EL, Cuthbertson K, Endesh N, Rode B, Blythe NM, Hyman AJ, Hall SJ, Gaunt HJ, Ludlow MJ, Foster R and Beech DJ. Yoda1 analogue (Dooku1) which antagonizes Yoda1-evoked activation of Piezo1 and aortic relaxation. Br J Pharmacol. 2018;175:1744–1759. [PubMed: 29498036]
16. Lacroix JJ, Botello-Smith WM and Luo Y. Probing the gating mechanism of the mechanosensitive channel Piezo1 with the small molecule Yoda1. Nat Commun. 2018;9:2029. [PubMed: 29795280]
17. Chubinskiy-Nadezhdin VI, Vasileva VY, Vassilieva IO, Sudarikova AV, Morachevskaya EA and Negulyaev YA. Agonist-induced Piezo1 activation suppresses migration of transformed fibroblasts. Biochem Biophys Res Commun. 2019;514:173–179. [PubMed: 31029419]
18. Jetta D, Gottlieb PA, Verma D, Sachs F and Hua SZ. Shear stress-induced nuclear shrinkage through activation of Piezo1 channels in epithelial cells. J Cell Sci. 2019;132.

19. Kang H, Hong Z, Zhong M, Klomp J, Bayless KJ, Mehta D, Karginov AV, Hu G and Malik AB. Piezo1 mediates angiogenesis through activation of MT1-MMP signaling. Am J Physiol Cell Physiol. 2019;316:C92–C103. [PubMed: 30427721]

20. Liu S, Pan X, Cheng W, Deng B, He Y, Zhang L, Ning Y and Li J. Tubeimoside I Antagonizes Yoda1-Evoked Piezo1 Channel Activation. Front Pharmacol. 2020;11:768. [PubMed: 32523536]

21. Wang YY, Zhang H, Ma T, Lu Y, Xie HY, Wang W, Ma YH, Li GH and Li YW. Piezo1 mediates neuron oxygen-glucose deprivation/reoxygenation injury via Ca(2+)/calpain signaling. Biochem Biophys Res Commun. 2019;513:147–153. [PubMed: 30948157]

22. Choi D, Park E, Jung E, Cha B, Lee S, Yu J, Kim PM, Lee S, Hong YJ, Koh CJ, Cho CW, Wu Y, Li Jeon N, Wong AK, Shin L, Kumar SR, Bermejo-Moreno I, Srinivasan RS, Cho IT and Hong YK. Piezo1 incorporates mechanical force signals into the genetic program that governs lymphatic valve development and maintenance. JCI Insight. 2019;4.

23. Wang S, Chennupati R, Kaur H, Iring A, Wettschureck N and Offermanns S. Endothelial cation channel PIEZO1 controls blood pressure by mediating flow-induced ATP release. J Clin Invest. 2016;126:4527–4536. [PubMed: 27797339]

24. Iring A, Jin YJ, Albarran-Juarez J, Siragusa M, Wang S, Dancs PT, Nakayama A, Tonack S, Chen M, Kunne C, Sokol AM, Gunther S, Martinez A, Fleming I, Wettschureck N, Graumann J, Weinstein LS and Offermanns S. Shear stress-induced endothelial adrenomedullin signaling regulates vascular tone and blood pressure. J Clin Invest. 2019;129:2775–2791. [PubMed: 31205027]

25. Ranade SS, Qiu Z, Woo SH, Hur SS, Murthy SE, Cahalan SM, Xu J, Mathur J, Bandell M, Coste B, Li YS, Chien S and Patapoutian A. Piezo1, a mechanically activated ion channel, is required for vascular development in mice. Proc Natl Acad Sci U S A. 2014;111:10347–52. [PubMed: 24958852]

26. Hyman AJ, Tumova S and Beech DJ. Piezo1 Channels in Vascular Development and the Sensing of Shear Stress. Curr Top Membr. 2017;79:37–57. [PubMed: 28728823]

27. Rode B, Shi J, Endesh N, Drinkhill MJ, Webster PJ, Lotteau SJ, Bailey MA, Yuldasheva NY, Ludlow MJ, Cubbon RM, Li J, Futers TS, Morley L, Gaunt HJ, Marszalek K, Viswambharan H, Cuthbertson K, Baxter PD, Foster R, Sukumar P, Weightman A, Calaghan SC, Wheatcroft SB, Kearney MT and Beech DJ. Piezo1 channels sense whole body physical activity to reset cardiovascular homeostasis and enhance performance. Nat Commun. 2017;8:350. [PubMed: 28839146]

28. Nonomura K, Lukacs V, Sweet DT, Goddard LM, Kanie A, Whitwam T, Ranade SS, Fujimori T, Kahn ML and Patapoutian A. Mechanically activated ion channel PIEZO1 is required for lymphatic valve formation. Proc Natl Acad Sci U S A. 2018;115:12817–12822. [PubMed: 30482854]

29. Lukacs V, Mathur J, Mao R, Bayrak-Toydemir P, Procter M, Cahalan SM, Kim HJ, Bandell M, Longo N, Day RW, Stevenson DA, Patapoutian A and Krock BL. Impaired PIEZO1 function in patients with a novel autosomal recessive congenital lymphatic dysplasia. Nat Commun. 2015;6:8329. [PubMed: 26387913]

30. Fotiou E, Martin-Almedina S, Simpson MA, Lin S, Gordon K, Brice G, Atton G, Jeffery I, Rees DC, Mignot C, Vogt J, Homfray T, Snyder MP, Rockson SG, Jeffery S, Mortimer PS, Mansour S and Ostergaard P. Novel mutations in PIEZO1 cause an autosomal recessive generalized lymphatic dysplasia with non-immune hydrops fetalis. Nat Commun. 2015;6:8085. [PubMed: 26333996]

31. Givens C and Tzima E. Endothelial Mechanosignaling: Does One Sensor Fit All? Antioxid Redox Signal. 2016;25:373–88. [PubMed: 27027326]

32. Gonzalez-Loyola A, Bovay E, Kim J, Lozano TW, Sabine A, Renevey F, Arroz-Madeira S, Rapin A, Wypych TP, Rota G, Durot S, Velin D, Marsland B, Guarda G, Delorenzi M, Zamboni N, Luther SA and Petrova TV. FOXC2 controls adult lymphatic endothelial specialization, function, and gut lymphatic barrier preventing multiorgan failure. Sci Adv. 2021;7.

33. Li X, Zhang Z, Han M, Li Y, He L and Zhou B. Generation of Piezo1-CreER transgenic mice for visualization and lineage tracing of mechanical force responsive cells in vivo. Genesis. 2022:e23476. [PubMed: 35500107]

34. Daigle TL, Madisen L, Hage TA, Valley MT, Knoblich U, Larsen RS, Takeno MM, Huang L, Gu H, Larsen R, Mills M, Bosma-Moody A, Siverts LA, Walker M, Graybuck LT, Yao Z, Fong O,

Nguyen TN, Garren E, Lenz GH, Chavarha M, Pendergraft J, Harrington J, Hirokawa KE, Harris JA, Nicovich PR, McGraw MJ, Ollerenshaw DR, Smith KA, Baker CA, Ting JT, Sunkin SM, Lecoq J, Lin MZ, Boyden ES, Murphy GJ, da Costa NM, Waters J, Li L, Tasic B and Zeng H. A Suite of Transgenic Driver and Reporter Mouse Lines with Enhanced Brain-Cell-Type Targeting and Functionality. Cell. 2018;174:465–480 e22. [PubMed: 30007418]

35. Azimi I, Stevenson RJ, Zhang X, Meizoso-Huesca A, Xin P, Johnson M, Flanagan JU, Chalmers SB, Yoast RE, Kapure JS, Ross BP, Vetter I, Ashton MR, Launikonis BS, Denny WA, Trebak M and Monteith GR. A new selective pharmacological enhancer of the Orai1 Ca(2+) channel reveals roles for Orai1 in smooth and skeletal muscle functions. ACS Pharmacol Transl Sci. 2020;3:135–147. [PubMed: 32190822]
36. Bazigou E, Lyons OT, Smith A, Venn GE, Cope C, Brown NA and Makinen T. Genes regulating lymphangiogenesis control venous valve formation and maintenance in mice. J Clin Invest. 2011;121:2984–92. [PubMed: 21765212]
37. Cahalan SM, Lukacs V, Ranade SS, Chien S, Bandell M and Patapoutian A. Piezo1 links mechanical forces to red blood cell volume. Elife. 2015;4.
38. Wani MA, Means RT, Jr. and Lingrel JB. Loss of LKLF function results in embryonic lethality in mice. Transgenic Res. 1998;7:229–38. [PubMed: 9859212]
39. Venkatesh DA, Park KS, Harrington A, Miceli-Libby L, Yoon JK and Liaw L. Cardiovascular and hematopoietic defects associated with Notch1 activation in embryonic Tie2-expressing populations. Circ Res. 2008;103:423–31. [PubMed: 18617694]
40. Hong M, Jung E, Yang S, Jung W, Seong YJ, Park E, Bramos A, Kim KE, Lee S, Daghlian G, Seo JI, Choi I, Choi IS, Koh CJ, Kobielak A, Ying QL, Johnson M, Gardner D, Wong AK, Choi D and Hong YK. Efficient Assessment of Developmental, Surgical and Pathological Lymphangiogenesis Using a Lymphatic Reporter Mouse and Its Embryonic Stem Cells. PLoS ONE. 2016;11:e0157126. [PubMed: 27280889]
41. Nosyreva ED, Thompson D and Syeda R. Identification and functional characterization of the Piezo1 channel pore domain. J Biol Chem. 2021;296:100225. [PubMed: 33361157]
42. Lee Y, Choi JW, Yu J, Park D, Ha J, Son K, Lee S, Chung M, Kim HY and Jeon NL. Microfluidics within a well: an injection-molded plastic array 3D culture platform. Lab Chip. 2018;18:2433–2440. [PubMed: 29999064]
43. Choi I, Chung HK, Ramu S, Lee HN, Kim KE, Lee S, Yoo J, Choi D, Lee YS, Aguilar B and Hong Y-K. Visualization of lymphatic vessels by Prox1-promoter directed GFP reporter in a bacterial artificial chromosome-based transgenic mouse. Blood. 2011;117:362–5. [PubMed: 20962325]
44. Wu Y, Seong YJ, Kin L, Choi D, Park E, Daghlian G, Jung E, Bui K, Luping Z, Madhavan S, Saren D, Patill D, Chin D, Cho I-T, Wong A, Heur M, Zhang-Nunes S, Tan J, Ema M, Wong TT, Huang AS and Hong Y-K. Organogenesis and Distribution of the Ocular Lymphatic Vessels in the Anterior Eye. JCI Insight. 2020.
45. Akiyama G, Saraswathy S, Bogarin T, Pan X, Barron E, Wong TT, Kaneko MK, Kato Y, Hong Y and Huang AS. Functional, structural, and molecular identification of lymphatic outflow from subconjunctival blebs. Exp Eye Res. 2020;196:108049. [PubMed: 32387381]
46. Rutkowski JM, Moya M, Johannes J, Goldman J and Swartz MA. Secondary lymphedema in the mouse tail: Lymphatic hyperplasia, VEGF-C upregulation, and the protective role of MMP-9. Microvasc Res. 2006;72:161–71. [PubMed: 16876204]
47. Choi I, Lee S, Kyoung Chung H, Suk Lee Y, Eui Kim K, Choi D, Park EK, Yang D, Ecoiffier T, Monahan J, Chen W, Aguilar B, Lee HN, Yoo J, Koh CJ, Chen L, Wong AK and Hong YK. 9-cis retinoic Acid promotes lymphangiogenesis and enhances lymphatic vessel regeneration: therapeutic implications of 9-cis retinoic Acid for secondary lymphedema. Circulation. 2012;125:872–82. [PubMed: 22275501]
48. Avraham T, Zampell JC, Yan A, Elhadad S, Weitman ES, Rockson SG, Bromberg J and Mehrara BJ. Th2 differentiation is necessary for soft tissue fibrosis and lymphatic dysfunction resulting from lymphedema. Faseb J. 2013;27:1114–26. [PubMed: 23193171]
49. Prakriya M, Feske S, Gwack Y, Srikanth S, Rao A and Hogan PG. Orai1 is an essential pore subunit of the CRAC channel. Nature. 2006;443:230–3. [PubMed: 16921383]

50. Yoast RE, Emrich SM and Trebak M. The anatomy of native CRAC channel(s). Curr Opin Physiol. 2020;17:89–95. [PubMed: 32999945]
51. Dekker RJ, van Soest S, Fontijn RD, Salamanca S, de Groot PG, VanBavel E, Pannekoek H and Horrevoets AJ. Prolonged fluid shear stress induces a distinct set of endothelial cell genes, most specifically lung Kruppel-like factor (KLF2). Blood. 2002;100:1689–98. [PubMed: 12176889]
52. Wigle JT and Oliver G. Prox1 function is required for the development of the murine lymphatic system. Cell. 1999;98:769–78. [PubMed: 10499794]
53. Takeyama K, Aguiar RC, Gu L, He C, Freeman GJ, Kutok JL, Aster JC and Shipp MA. The BAL-binding protein BBAP and related Deltex family members exhibit ubiquitin-protein isopeptide ligase activity. J Biol Chem. 2003;278:21930–7. [PubMed: 12670957]
54. Jahnsen ED, Trindade A, Zaun HC, Lehoux S, Duarte A and Jones EA. Notch1 is pan-endothelial at the onset of flow and regulated by flow. PLoS ONE. 2015;10:e0122622. [PubMed: 25830332]
55. Masumura T, Yamamoto K, Shimizu N, Obi S and Ando J. Shear stress increases expression of the arterial endothelial marker ephrinB2 in murine ES cells via the VEGF-Notch signaling pathways. Arterioscler Thromb Vasc Biol. 2009;29:2125–31. [PubMed: 19797707]
56. Sweet DT, Chen Z, Givens CS, Owens AP, Rojas M and Tzima E. Endothelial Shc regulates arteriogenesis through dual control of arterial specification and inflammation via the notch and nuclear factor-kappa-light-chain-enhancer of activated B-cell pathways. Circ Res. 2013;113:32–39. [PubMed: 23661718]
57. Caolo V, Debant M, Endesh N, Futers TS, Lichtenstein L, Bartoli F, Parsonage G, Jones EA and Beech DJ. Shear stress activates ADAM10 sheddase to regulate Notch1 via the Piezo1 force sensor in endothelial cells. Elife. 2020;9.
58. Alders M, Hogan BM, Gjini E, Salehi F, Al-Gazali L, Hennekam EA, Holmberg EE, Mannens MM, Mulder MF, Offerhaus GJ, Prescott TE, Schroor EJ, Verheij JB, Witte M, Zwijnenburg PJ, Vikkula M, Schulte-Merker S and Hennekam RC. Mutations in CCBE1 cause generalized lymph vessel dysplasia in humans. Nat Genet. 2009;41:1272–4. [PubMed: 19935664]
59. Alders M, Al-Gazali L, Cordeiro I, Dallapiccola B, Garavelli L, Tuysuz B, Salehi F, Haagmans MA, Mook OR, Majoie CB, Mannens MM and Hennekam RC. Hennekam syndrome can be caused by FAT4 mutations and be allelic to Van Maldergem syndrome. Hum Genet. 2014;133:1161–7. [PubMed: 24913602]
60. Lee W, Leddy HA, Chen Y, Lee SH, Zelenski NA, McNulty AL, Wu J, Beicker KN, Coles J, Zauscher S, Grandl J, Sachs F, Guilak F and Liedtke WB. Synergy between Piezo1 and Piezo2 channels confers high-strain mechanosensitivity to articular cartilage. Proc Natl Acad Sci U S A. 2014;111:E5114–22. [PubMed: 25385580]
61. Retailleau K, Arhatte M, Demolombe S, Peyronnet R, Baudrie V, Jodar M, Bourreau J, Henrion D, Offermanns S, Nakamura F, Feng Y, Patel A, Duprat F and Honore E. Arterial Myogenic Activation through Smooth Muscle Filamin A. Cell Rep. 2016;14:2050–2058. [PubMed: 26923587]
62. Wang S, Iring A, Strilic B, Albarran Juarez J, Kaur H, Troidl K, Tonack S, Burbiel JC, Muller CE, Fleming I, Lundberg JO, Wettschureck N and Offermanns S. P2Y(2) and Gq/G(1)(1) control blood pressure by mediating endothelial mechanotransduction. J Clin Invest. 2015;125:3077–86. [PubMed: 26168216]
63. Zhang T, Chi S, Jiang F, Zhao Q and Xiao B. A protein interaction mechanism for suppressing the mechanosensitive Piezo channels. Nat Commun. 2017;8:1797. [PubMed: 29176668]
64. Soboloff J, Rothberg BS, Madesh M and Gill DL. STIM proteins: dynamic calcium signal transducers. Nat Rev Mol Cell Biol. 2012;13:549–65. [PubMed: 22914293]
65. McHugh BJ, Buttery R, Lad Y, Banks S, Haslett C and Sethi T. Integrin activation by Fam38A uses a novel mechanism of R-Ras targeting to the endoplasmic reticulum. J Cell Sci. 2010;123:51–61. [PubMed: 20016066]
66. Satoh K, Hata M, Takahara S, Tsuzaki H, Yokota H, Akatsu H, Yamamoto T, Kosaka K and Yamada T. A novel membrane protein, encoded by the gene covering KIAA0233, is transcriptionally induced in senile plaque-associated astrocytes. Brain Res. 2006;1108:19–27. [PubMed: 16854388]

67. Liao J, Lu W, Chen Y, Duan X, Zhang C, Luo X, Lin Z, Chen J, Liu S, Yan H, Chen Y, Feng H, Zhou D, Chen X, Zhang Z, Yang Q, Liu X, Tang H, Li J, Makino A, Yuan JX, Zhong N, Yang K and Wang J. Upregulation of Piezo1 (Piezo Type Mechanosensitive Ion Channel Component 1) Enhances the Intracellular Free Calcium in Pulmonary Arterial Smooth Muscle Cells From Idiopathic Pulmonary Arterial Hypertension Patients. Hypertension. 2021;77:1974–1989. [PubMed: 33813851]

68. Baluk P and McDonald DM. Imaging Blood Vessels and Lymphatics in Mouse Trachea Wholemounts. Methods Mol Biol. 2022;2441:115–134. [PubMed: 35099733]

69. Bramos A, Perrault D, Yang S, Jung E, Hong YK and Wong AK. Prevention of Postsurgical Lymphedema by 9-cis Retinoic Acid. Ann Surg. 2016;264:353–61. [PubMed: 26655920]

Novelty and Significance

What Is Known?

- Tissue fluid build-up and increased interstitial pressure coincide with embryonic lymphatic development.
- Shear stress generated by fluid flow brings two opposing consequences to blood and lymphatic vessels: growth arrest and growth activation.
- Shear stress activates calcium entry in lymphatic endothelial cells through the Store Operated Calcium Entry (SOCE) mechanism, which leads to Notch-downregulation and consequential lymphatic sprouting.

What new information does this article contribute?

- Piezo1 senses the shear stress and activates the SOCE mechanism.
- Genetic or pharmacological stimulation of Piezo1 triggers lymphatic sprouting.
- This mechanism can be therapeutically applicable to prevent surgery-associated lymphedema.

Lymphatics drain tissue fluid, and a high tissue fluid level activates lymphatic growth. However, the underlying mechanism remained unknown. Our study aimed to define the molecular basis for fluid flow-induced lymphatic expansion. We found that Piezo1 plays a critical molecular sensor in lymphatic endothelial cells that senses the fluid flow-generated force and increases the intracellular calcium influx. Increased calcium entry downregulates Notch, consequentially lymphatic sprouting. Genetic or pharmacological activation of Piezo1 efficiently ameliorates surgery-associated lymphedema by increasing lymphatic regeneration. Together, our study provides the molecular basis for flow-induced lymphatic expansion and offers a novel therapeutic concept against lymphedema.

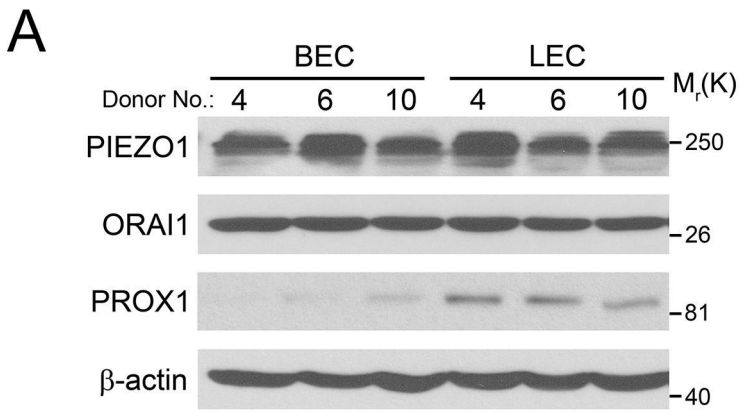

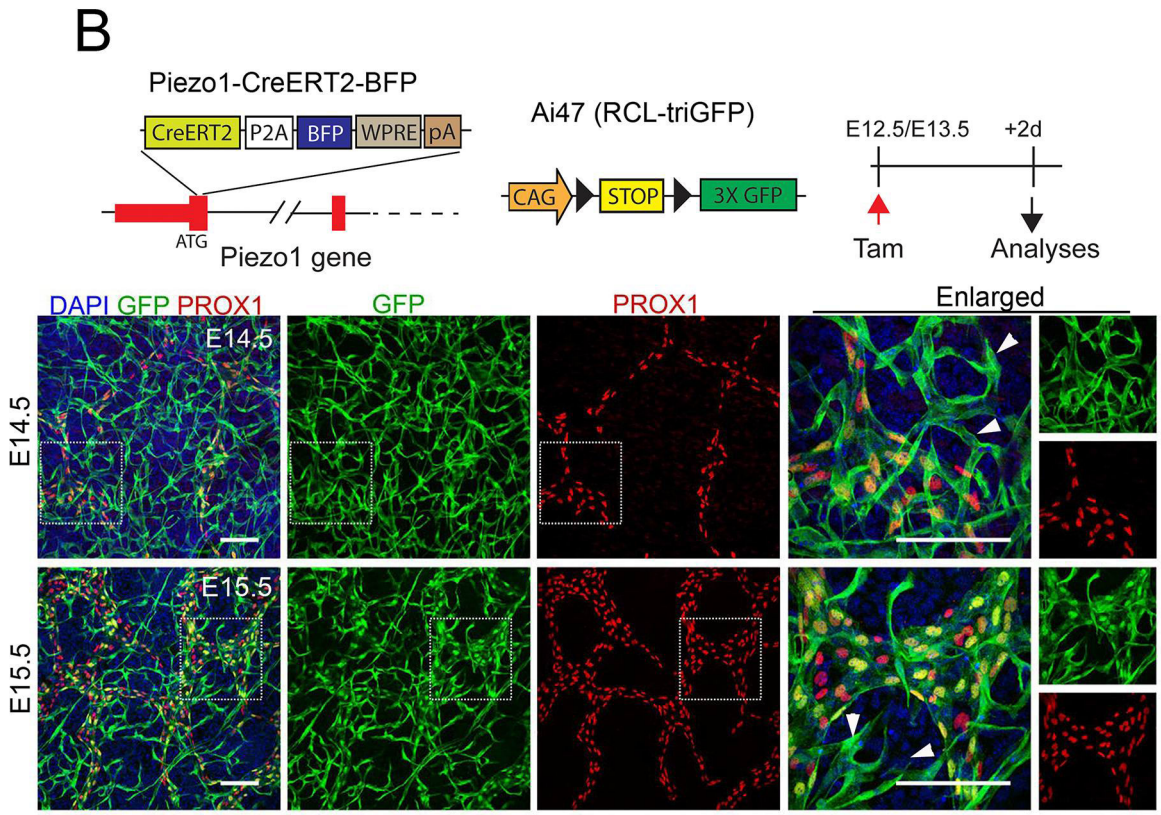

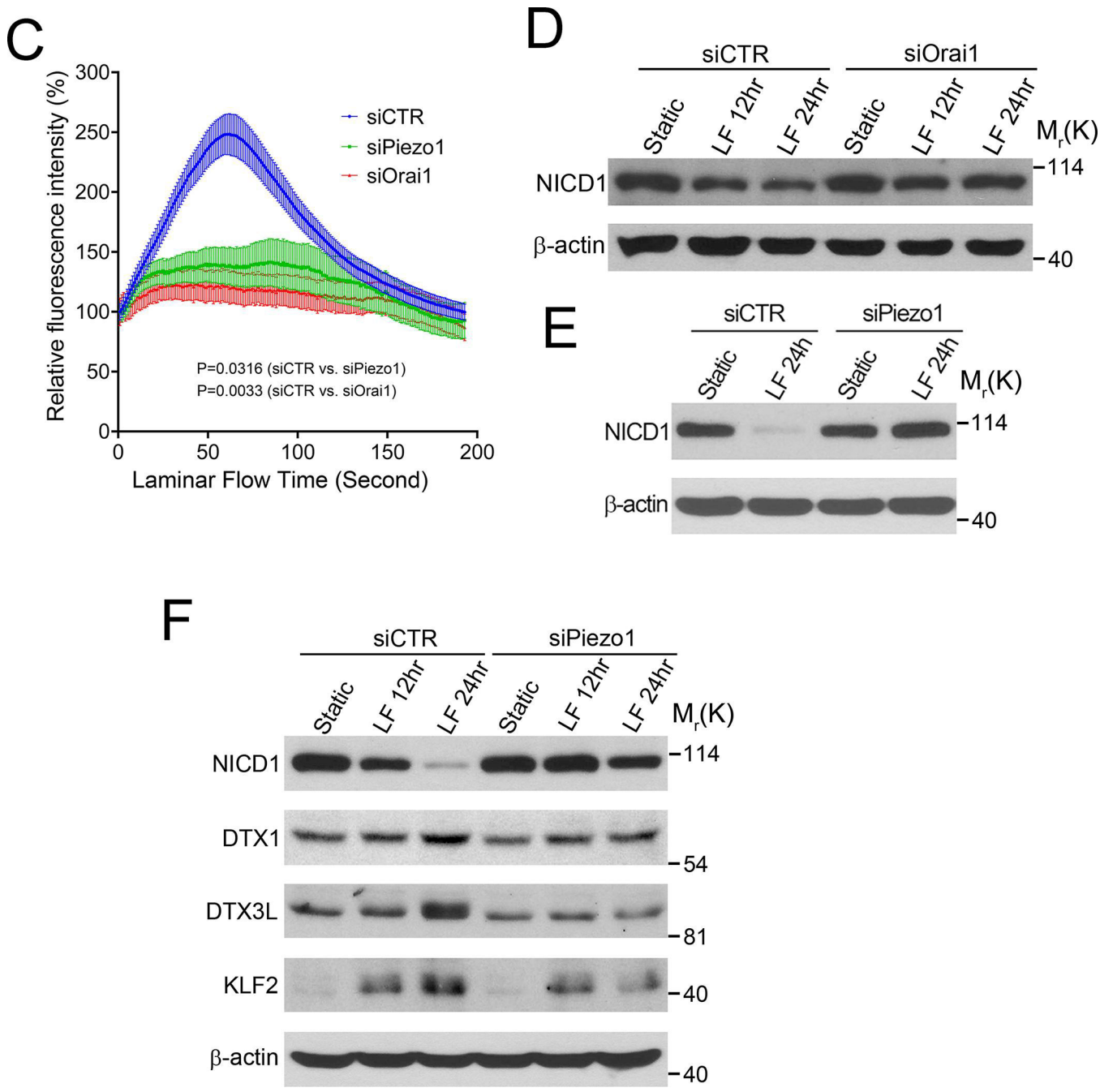

Figure 1. Piezo1 Is Required for Flow-Activated Notch Downregulation

(**A**) Western blot analyses showing the expression of Piezo1, Orai1, Prox1, and β-actin in three sets of the same donor-derived BECs and LECs. (**B**) Detection of endogenous Piezo1 expression in developing lymphatics using a novel Piezo1 reporter mouse with Piezo1-CreER^{T2}-BFP (blue fluorescence protein) driver allele and Ai47 (CAG-LSL-3XGFP) [34] reporter allele. The Piezo1-CreER^{T2}-BFP driver was created by CRISPR/Cas9-mediated insertion of a DNA cassette (CreER^{T2}-P2A-BFP-WPRE-polyA) immediately following the ATG initiation codon in the endogenous Piezo1, allowing CreER^{T2} and BFP to mirror the endogenous Piezo1expression pattern. Tamoxifen (6 mg) was injected into pregnant females

bearing Piezo1 reporter embryos at E12.5 or E13.5. After two days, embryos were harvested at E14.5 or E15.5, respectively. Embryonic back skins were stained with an anti-Prox1 antibody to detect lymphatic vessels. White arrows indicate Prox1-negative blood vessels. Scale bars: 100 μm. (**C**) Flow-activated calcium influx is blocked by knockdown of Piezo1 or Orai1 in LECs. Cells were transfected with Piezo1 siRNA (siPiezo1), Orai1 siRNA (siOrai1), or scrambled siRNA (siCTR) for 24 hours and then subjected to laminar flow (2 dyne/cm^2) [5]. N=10 per group. Statistics: two-way repeated-measures ANOVA. (**D, E**) Orai1 and Piezo1 knockdown similarly abrogated the flow-induced downregulation of NICD in LECs. Cells were transfected with the corresponding siRNA for 24-hours and subjected to laminar flow (LF, 2 dyne/cm^2) for 12- or 24-hours, or alternatively cultured under the static condition for 24 hours. (**F**) Piezo1 knockdown in LECs abrogated the flow-induced regulation of Orai1 downstream genes such as Dtx1, Dtx3L, Klf2, and Notch1. Experiments were repeated at least three times.

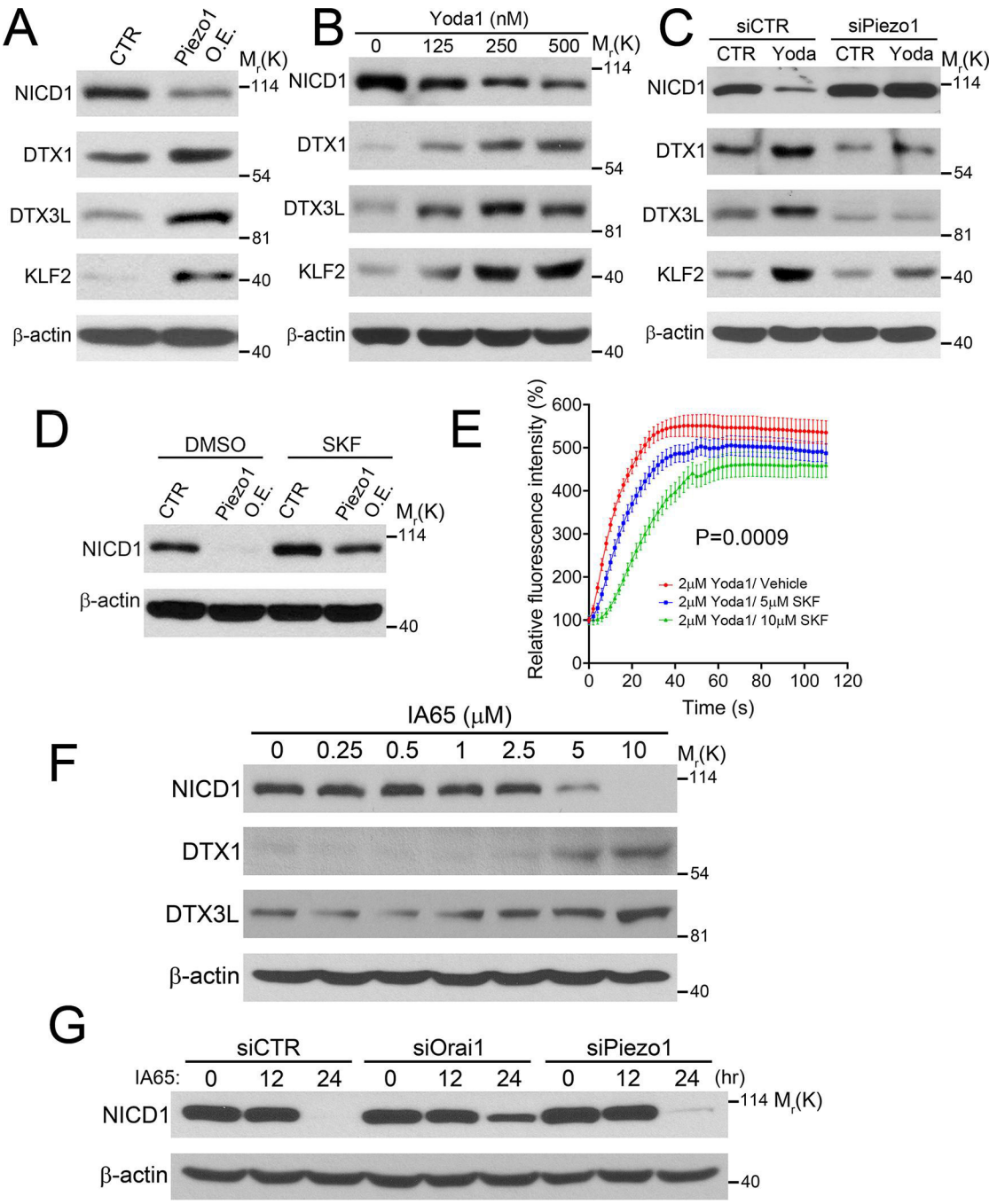

Figure 2. Piezo1 is a Mechanosensor for the Orai1-Regulated Notch Pathway.

(**A**) Piezo1 overexpression (O.E.) mimicked the flow-mediated regulation of NICD1, Dtx1, Dtx3L, and Klf2 in the absence of flow. LECs were transfected with a control vector or a mouse Piezo1-expressing vector for 48 hours before cells were harvested. (**B**) Yoda1 regulates the Orai1-downstream genes. LECs were treated with Yoda1 at the indicated concentrations for 24 hours under the static condition. (**C**) Regulation of Orai1 downstream genes by Yoda1 was inhibited by Piezo1 knockdown in LECs for 24 hours, followed by Yoda1 treatment (250 nM, 24 hours). (**D**) Orai1 inhibition abrogated the

NICD-downregulation caused by Piezo1 overexpression (O.E.). LECs were transfected with a control or a Piezo1 vector for 24 hours and then treated with an Orai1 inhibitor SKF-96365 (SKF, 10 nM) for 24 hours. (**E**) Orai1 inhibition suppressed Yoda1-activated calcium influx. LECs were loaded with a calcium dye (Fluo-4) and treated with SKF-96365 (SKF, 5 or 10 μM) for 10 minutes, followed by Yoda1 treatment (2 μM). N=10 per group. Statistics: two-way repeated-measures ANOVA. (**F**) An Orai1 agonist IA65 recapitulates the flow-mediated mechanotransduction phenotypes: NICD downregulation and Dtx1/Dtx3L upregulation. LECs were treated with IA65 at the indicated concentrations for 24 hours under the static condition. (**G**) NICD downregulation caused by IA65 treatment was suppressed by Orai1 knockdown but not by Piezo1 knockdown.

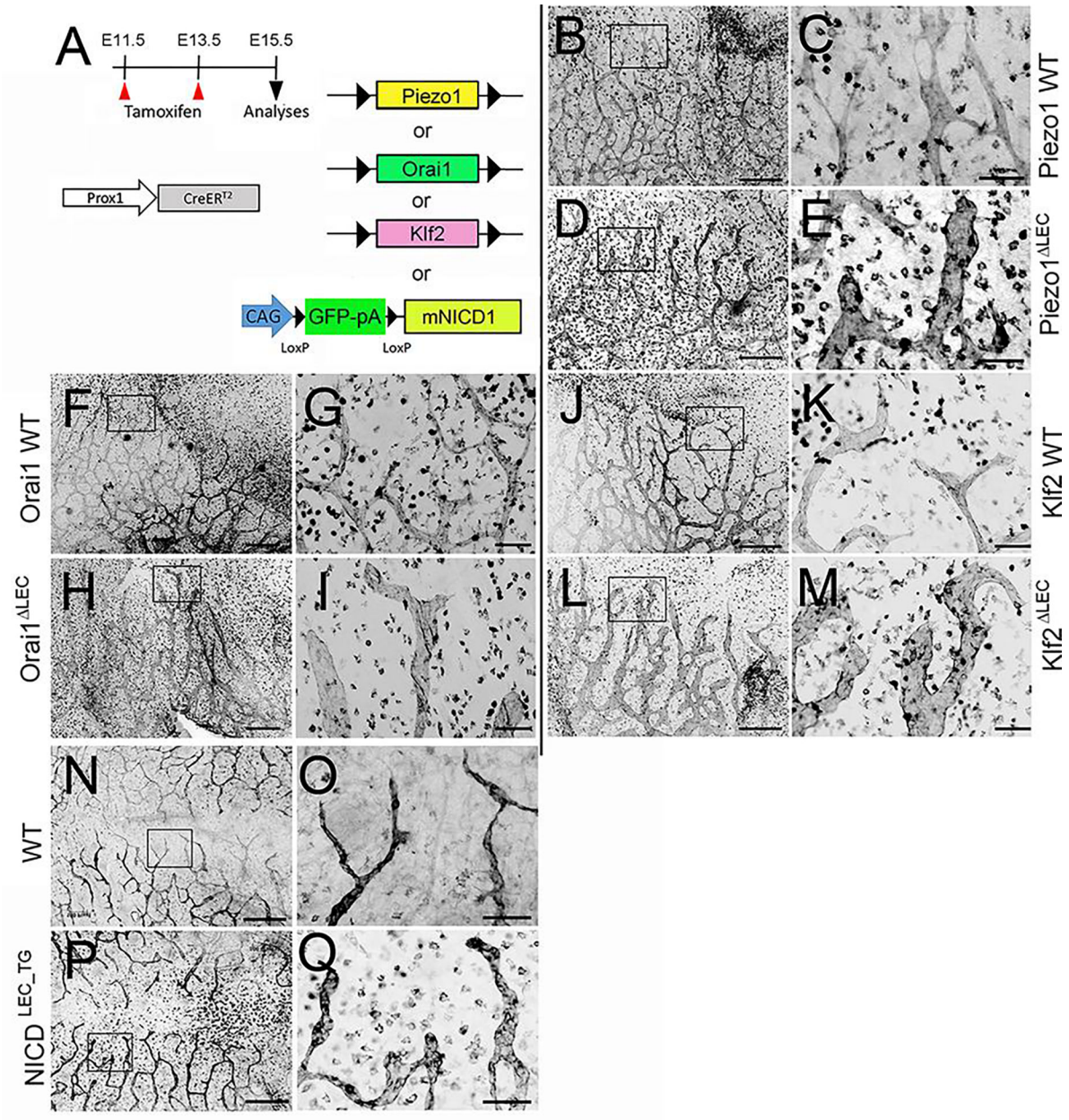

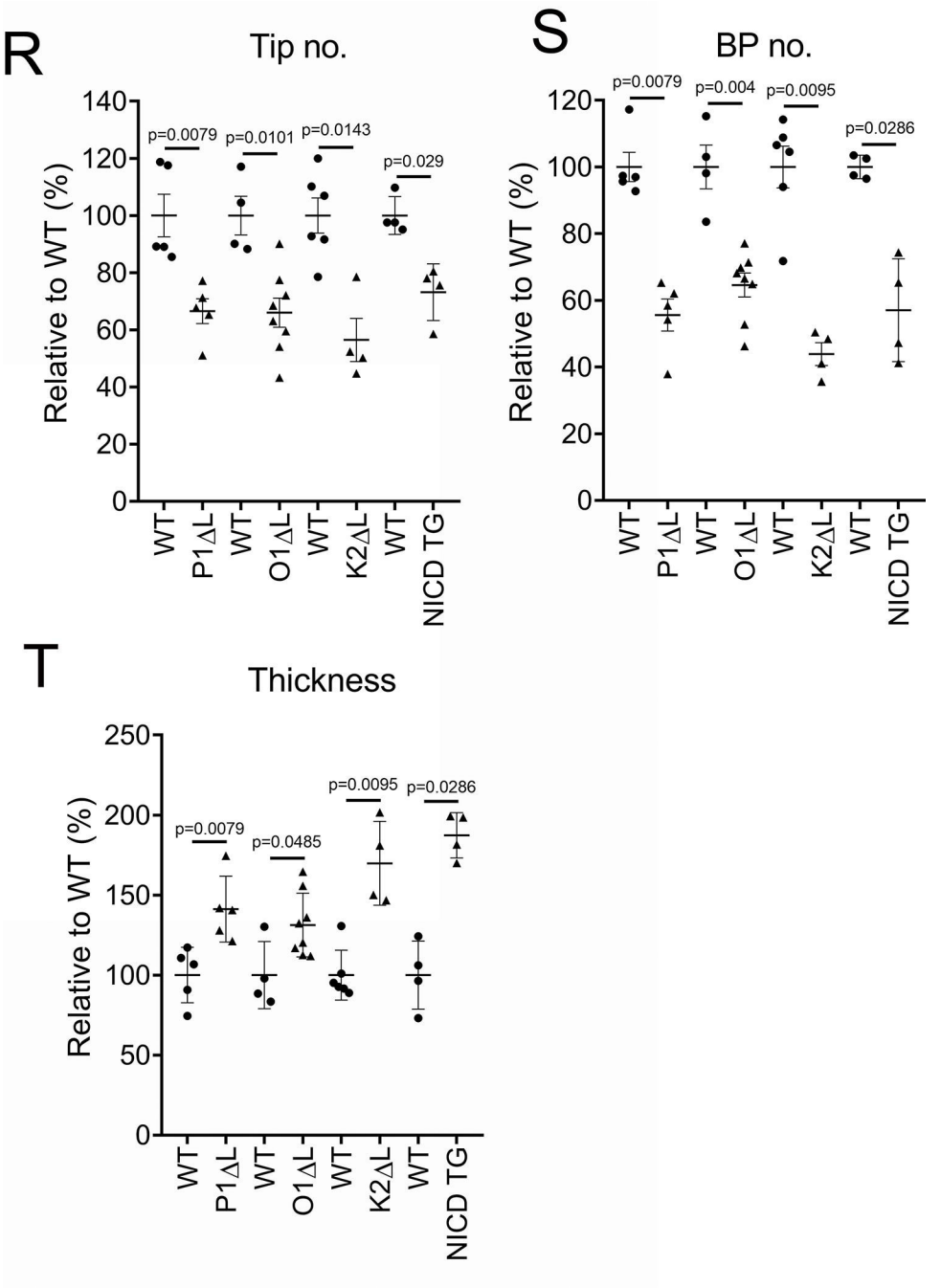

Figure 3. Piezo1 KO Phenocopies Lymphatic Defects of Orai1 KO, Klf2 KO, and NICD TG.

(**A**) Diagram showing lymphatic-specific conditional knockout or transgenic strategy for Piezo1, Orai1, Klf2, or NICD1. Defective lymphatic sprouting in embryonic back skins caused by lymphatic-specific deletion of Piezo1 (**B-E**), Orai1 (**F-I**), and Klf2 (**J-M**) or by ectopic NICD1 expression (**N-Q**), compared to their wild-type control littermates. Lymphatics were visualized by anti-Lyve1 whole-mount staining. Scale bars: 500 μm in B, D, F, H, J, L, N, and P; 100 μm in C, E, G, I, K, M, O, and Q. Graphs showing the relative numbers of lymphatic vessel tip (**R**), branches (**S**), and vessel thickness (**T**) in embryos

of wild-type (WT), lymphatic-specific Piezo1 (P1ΔL), Orai1 (O1ΔL), and Klf2 (K2ΔL) deletions, or NICD transgenic expression (NICD TG). Successful Cre-mediated genomic recombination was confirmed using PCR-based genotyping analyses (Figure S2). Embryos from multiple litters per group were analyzed (WT n=5 mice vs. P1ΔL n=5 mice, WT n=4 mice vs. O1ΔL n=8 mice, WT n=6 mice vs. K2ΔL n=4 mice, and WT n=4 mice vs. NICD TG n=4 mice). Statistics: Mann-Whitney *U* test.

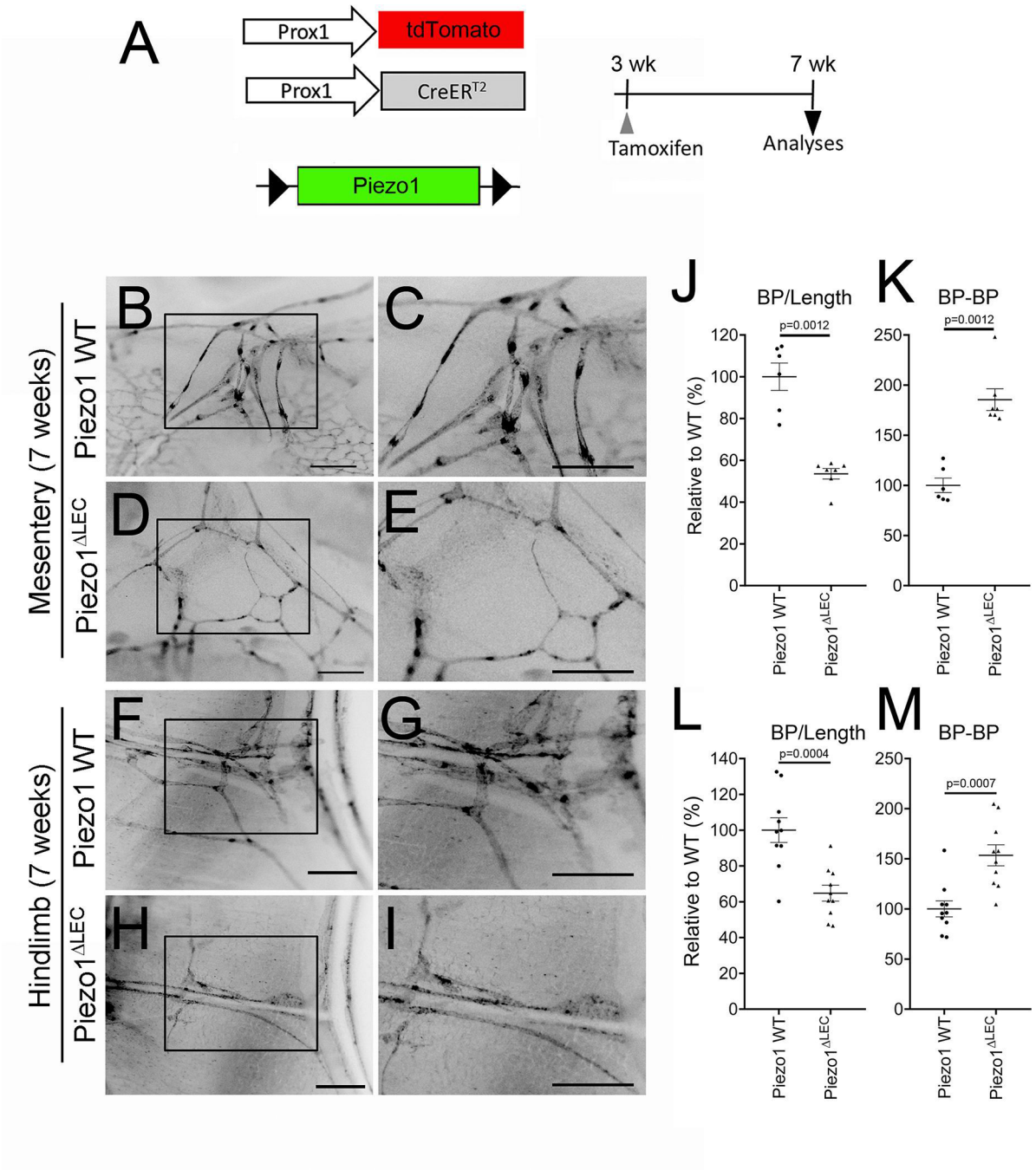

Figure 4. Piezo1 Is Required for Postnatal Lymphatic Development and Maintenance

(**A**) Diagram illustrating postnatal induction of lymphatic-specific Piezo1 KO. Tamoxifen was injected into the 3-week-old juvenile control or Piezo1$^{\Delta LEC}$ mice, followed by lymphatic analyses at 7 weeks. Lymphatics were visualized using Prox1-tdTomato reporter allele [40]. Lymphatic Piezo1 KO was induced in young adults (3 weeks old) by Tamoxifen injection at Days 21, 23, and 25. The colon mesentery (**B-E**) and hindlimb skins (**F-I**) were collected for lymphatic analyses at 7 weeks. Branch points per lymphatic vessel length (BP/Length) and distance between two branch points (BP-BP) were compared in the mesentery

(**J,K**) and hindlimb (**L,M**) between wild type and Piezo1$^{\Delta LEC}$ mice. Each dot represents one animal (WT n=6 mice vs. Piezo1$^{\Delta LEC}$ n=7 mice) (**J,K**), or one limb (n=10 mice per group) (**L,M**). Scale bars: 100 μm. Statistics: Mann-Whitney *U* test (**J** and **K**), and two-tailed *t*-test (**L** and **M**).

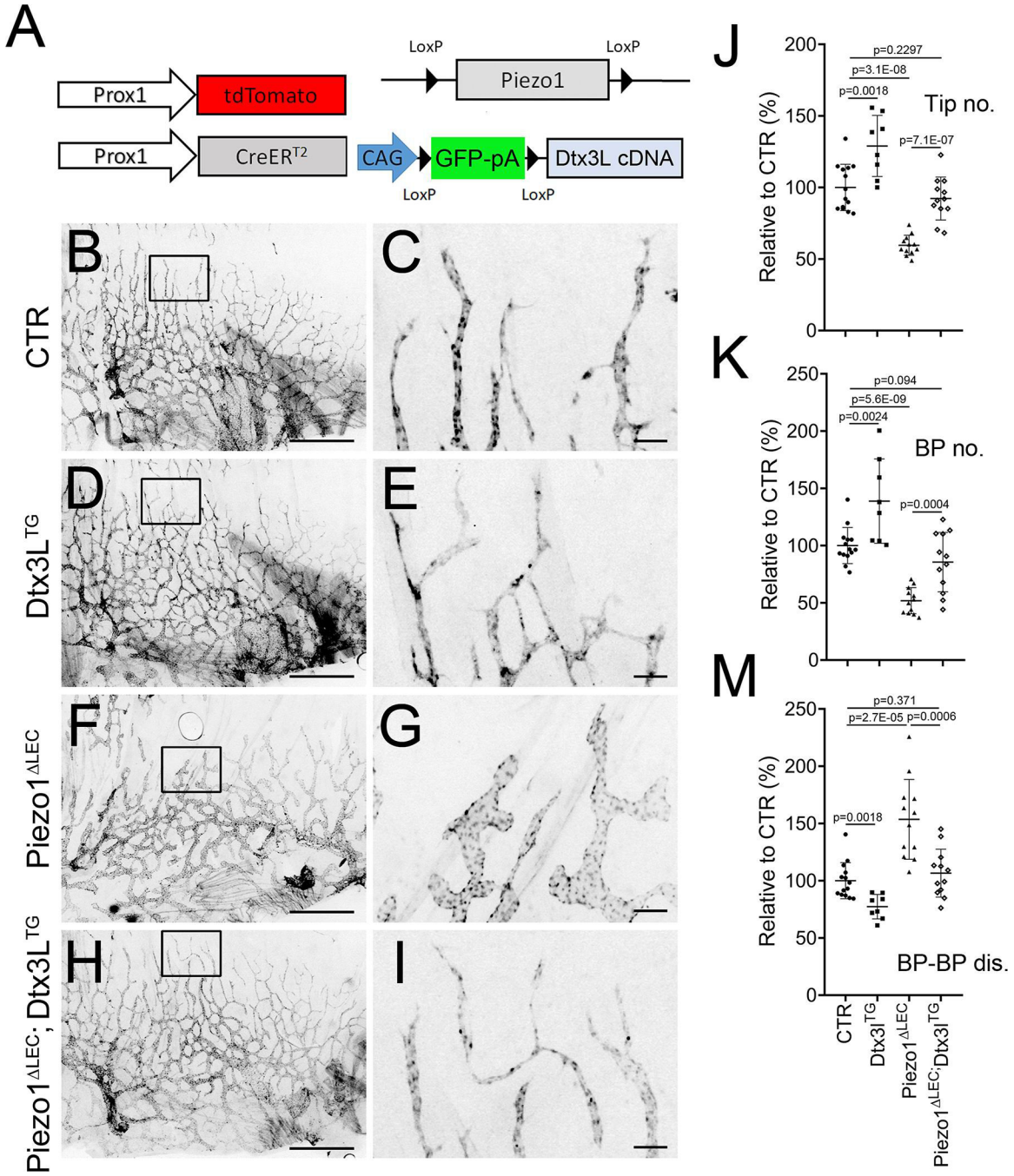

Figure 5. Dtx3L Overexpression Rescues Lymphatic Defects Caused by Piezo1 KO

(**A**) Genetic components of the mice for this experiment: Prox1-tdTomato, Prox1-CreER^{T2}, Piezo1 $^{fl/fl}$, and/or Dtx3L transgenic (TG) allele. pA, poly-A sequences. (**B-I**) Lymphatic vessels in control back skin (B,C), lymphatic-specific Dtx3L transgenic back skin (D,E), lymphatic-specific Piezo1 KO back skin (F,G), and lymphatic-specific Dtx3L transgenic/ Piezo1 KO back skin (H,I). Pregnant mice were injected with Tamoxifen at E11.5 and 13.5, and embryos were harvested at E15.5. Scale bars: 1 mm (B, D, F, H), 100 μm (C, E, G, I). (**J-M**) Graphs showing the percent changes in lymphatic tip number (J),

branch point number (BP No.) (K), and the distance between two branch points (BP-BP dis.) (M). Six different litters were analyzed (CTR n=14, $Dtx3l^{TG}$ n=8, $Piezo1^{\Delta LEC}$, n=12, and $Piezo1^{\Delta LEC}$; $Dtx3l^{TG}$ n=12 mice). Images in panel B-I were obtained from one representative litter. Lymphatic vessels were visualized by the Prox1-tdTomato reporter. Statistics: two-tailed *t*-test.

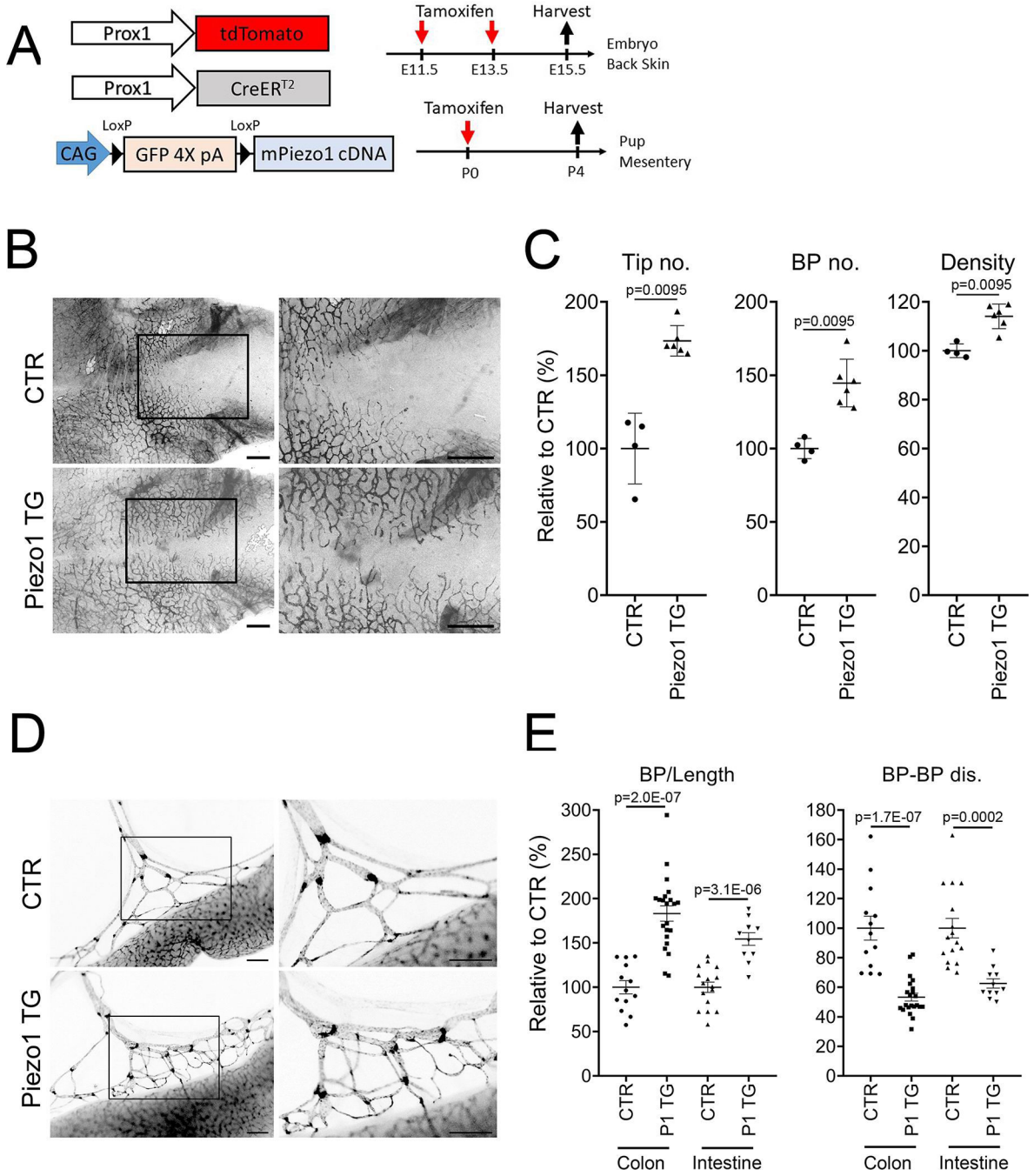

Figure 6. Transgenic Piezo1 Expression Promotes Lymphatic Sprouting and Network Formation

(**A**) Genetic components of the mice for this experiment: Prox1-tdTomato, Prox1-CreER^{T2}, and/or mouse Piezo1 cDNA transgenic (TG) allele. (**B, C**) Pregnant females were injected with Tamoxifen at E11.5 and 13.5, and their embryos were harvested at 15.5 for lymphatic analyses. Lymphatic vessel tip number (Tip no.), branch point (BP no.), and lymphatic density of Piezo1 ^{TG} embryos (n=6 mice) were compared to those of their control litter embryos (CTR, n=4 mice). (**D, E**) Alternatively, newborns (P0) were injected with Tamoxifen, and their mesenteries were harvested at P4. Mesenteric lymphatics in the colon

are shown (D). The number of branch points per lymphatic vessel length and distance between two branch points in the colon and intestine mesentery lymphatics of the control vs. Piezo1 ^{TG} pups (n=6 mice per group) (E). Each dot represents one bunch of mesentery lymphatic pre-collectors. Scale bars: 1 mm. Lymphatic vessels were visualized by the Prox1-tdTomato reporter. Statistics: Mann-Whitney *U* test (**C**), and two-tailed *t*-test (**E**).

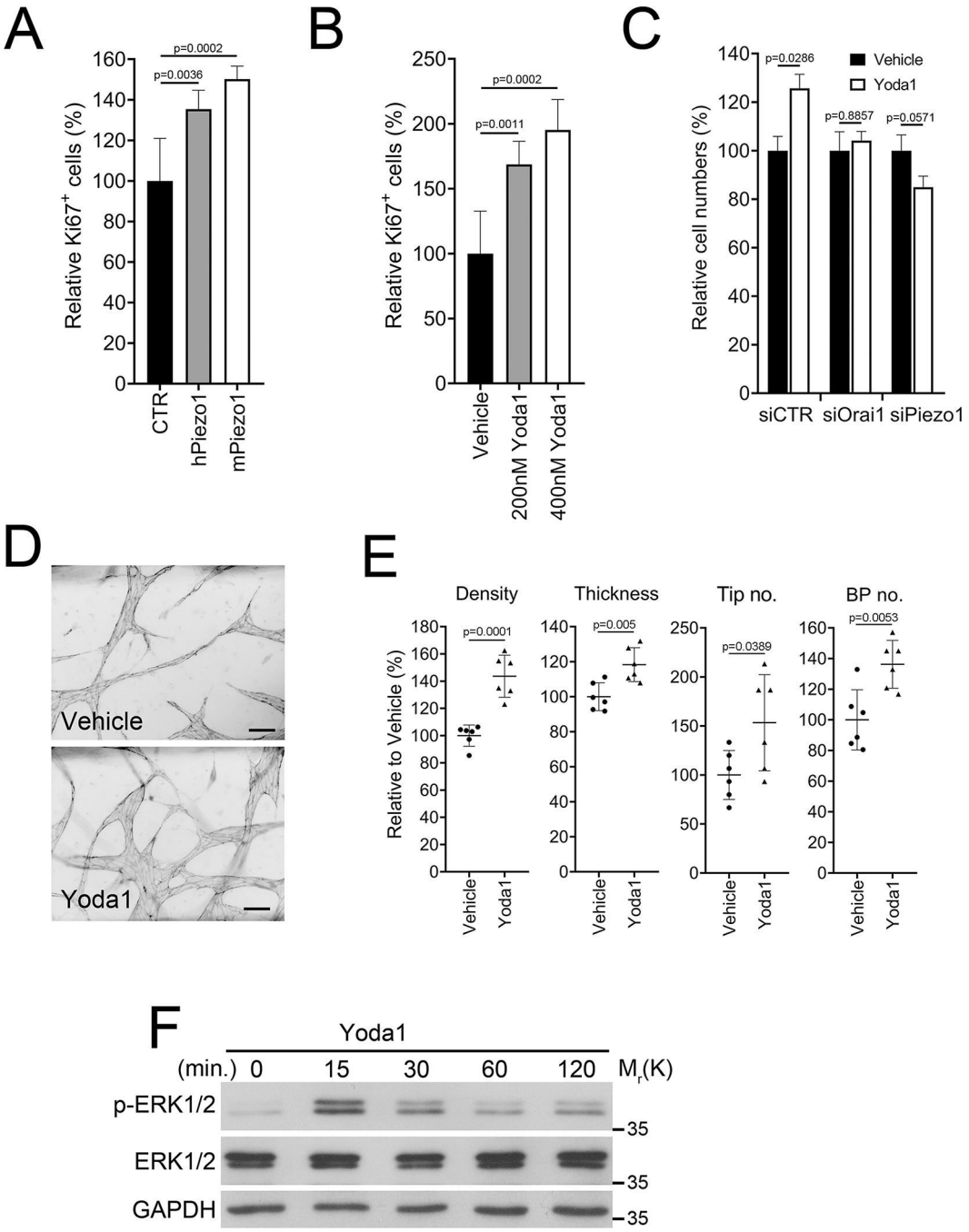

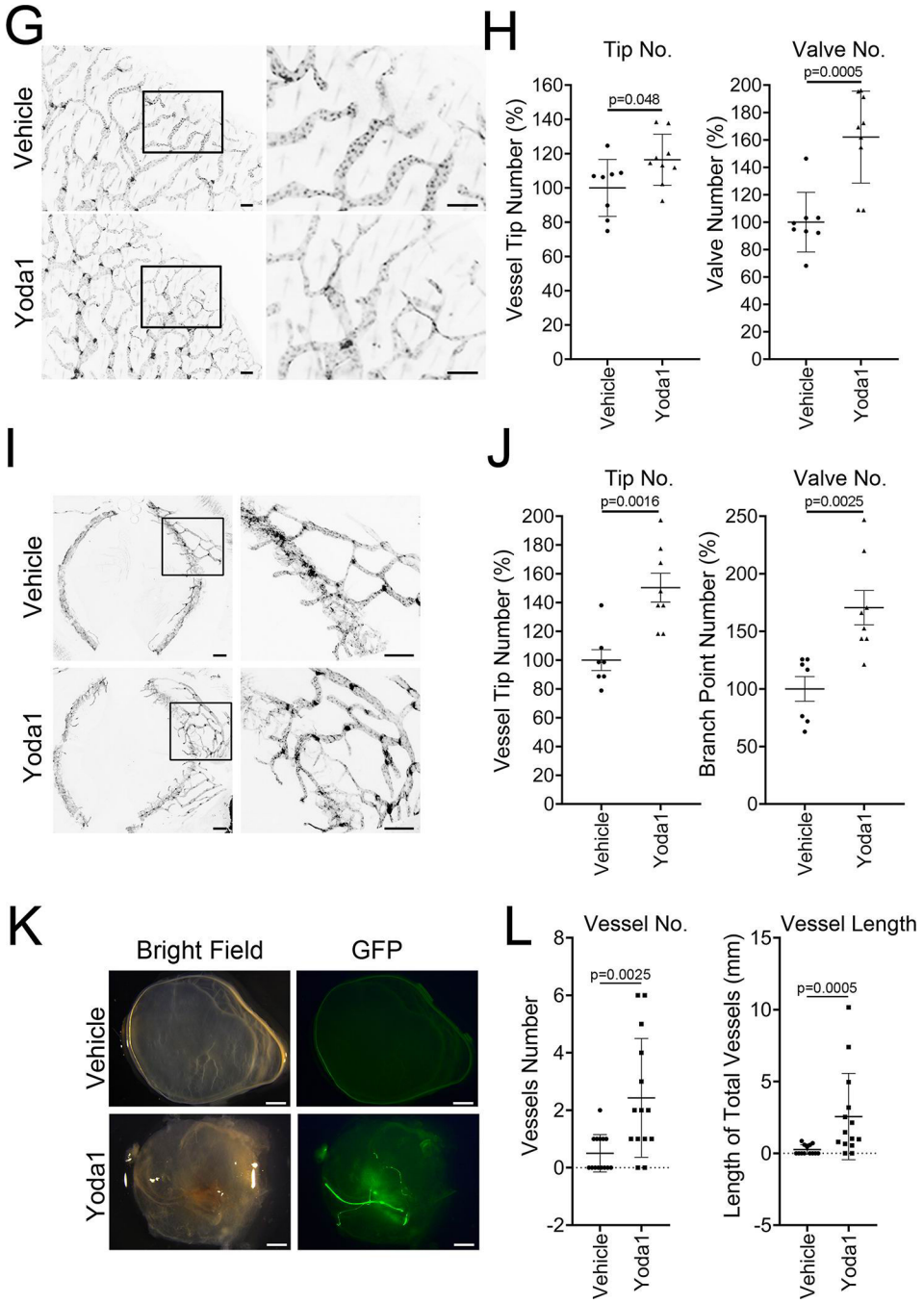

Figure 7. Piezo1 Activation Stimulates Lymphangiogenesis in Adults

(**A**) Primary LECs were transiently transfected with a control (CTR), human Piezo1-, or mouse Piezo1- vector for 48 hours and then subjected to Ki67 immunostaining (n=6 per group). (**B**) LECs were treated with vehicle or Yoda1 at 200 or 400 nM for 24 hours and subjected to Ki67 immunostaining (n=6 per group). (**C**) LECs were transiently transfected with siRNA for control (siCTR), Orai1 (siOrai1), or Piezo1 (siPiezo1). After 24 hours, cells were treated with vehicle or Yoda1 (300 nM) for 24 hours, followed by total cell number counting (n=4 per group). (**D**) The effect of Yoda1 on 3-D lymphatic network

formation was assessed. LECs are allowed to form 3-D lymphatic networks in fibrin gels containing vehicle or Yoda1 (500 nM) in a vessel-on-a-chip device [42]. After 3 days, lymphatic networks were fixed and stained against VE-Cadherin. Scale bars: 100 μm. (**E**) Morphometric analyses of the 3-D lymphatic vessels. BP, branch point (n=6 per group). (**F**) Western blots showing ERK1/2 phosphorylation in LECs treated with Yoda1 (400 nM) for the indicated time. The vehicle-treated sample is marked 0 minutes, and Glyceraldehyde-3-Phosphate Dehydrogenase (GAPDH) levels are also shown as loading controls. (**G**) Yoda1 activated dermal lymphangiogenesis in the mouse ears. These ears were harvested from mice subjected to the tail lymphedema model (Figure 8). Adult Prox1-EGFP lymphatic reporter mice were i.p. injected daily with vehicle or Yoda1 (71 μg/kg/day) over 35 days. (**H**) The numbers of lymphatic tips and valves were compared between the two groups (Vehicle n=8 and Yoda1 n=9 mice). (**I**) Yoda1 activated postnatal growth of the ocular lymphatics. Vehicle (10 μL, DMSO) or Yoda1 (10 μL, 50 μM in DMSO) was injected into the subconjunctival area of adult Prox-1-tdTomato mice every other day. The eyes were harvested 6 days after the first injection. (**J**) Numbers of lymphatic tip and valve were compared between the vehicle (n=7 mice) vs. Yoda1-injected groups (n=8 mice). (**K**) Matrigel matrix pre-mixed with vehicle or Yoda1 (500 nM) was intradermally injected into the flank of adult Prox1-EGFP mice. After two weeks, Matrigel plugs were harvested, and lymphatic ingrowth was visualized. Mouse VEGFC (50 ng/mL) was added to both groups to promote lymphatic expansion. 7 mice were used in each group. (**L**) Lymphatic vessels numbers and vessel length were compared between vehicle- vs. Yoda1-containing Matrigel plugs (n=14 Matrigel plugs per group). Scale bars: 200 μm in G and I; 500 μm in K. Statistics: Mann-Whitney *U* test (**C** and **L**), and two-tailed *t*-test (**A, B, E, H,** and **J**).

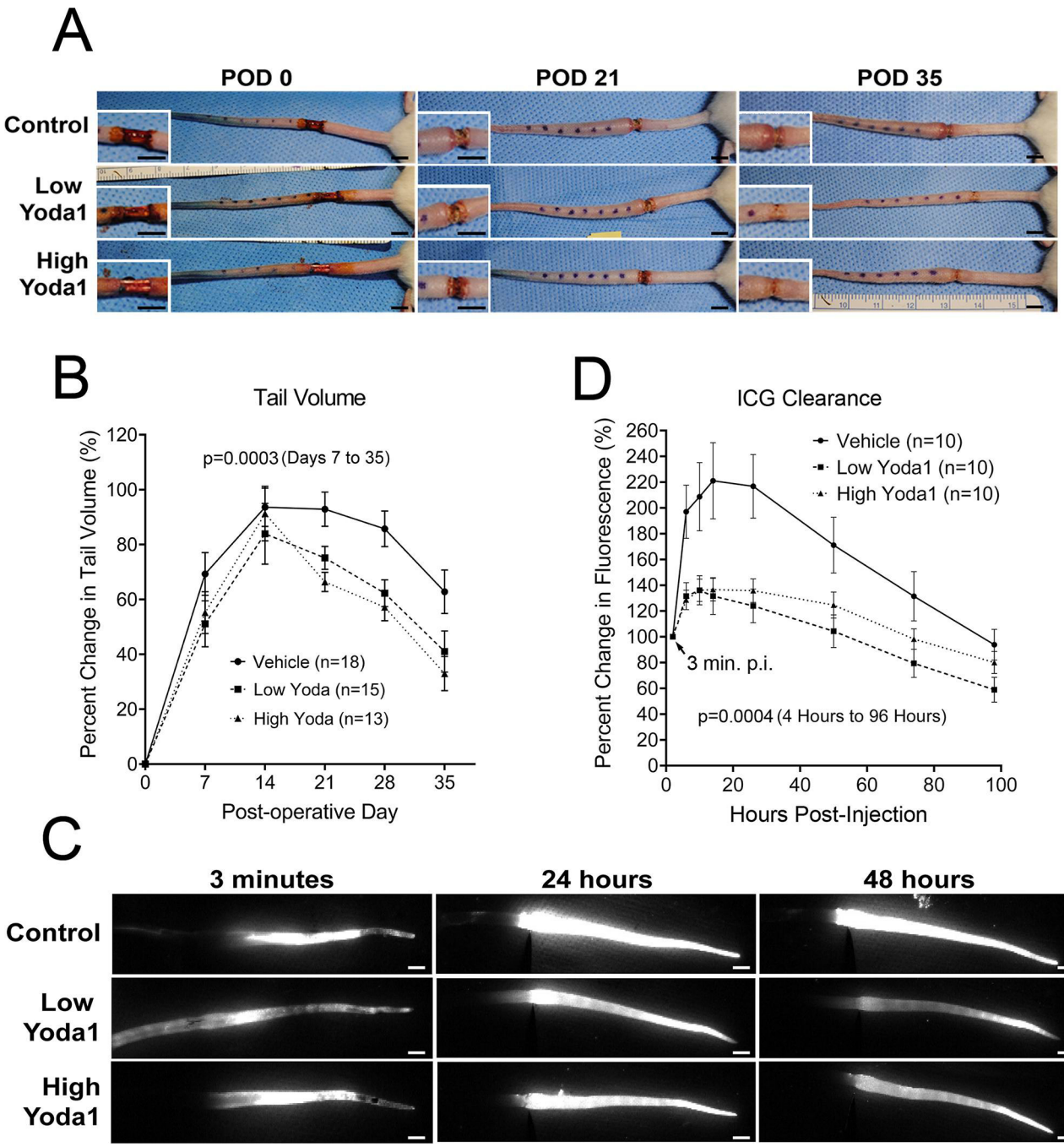

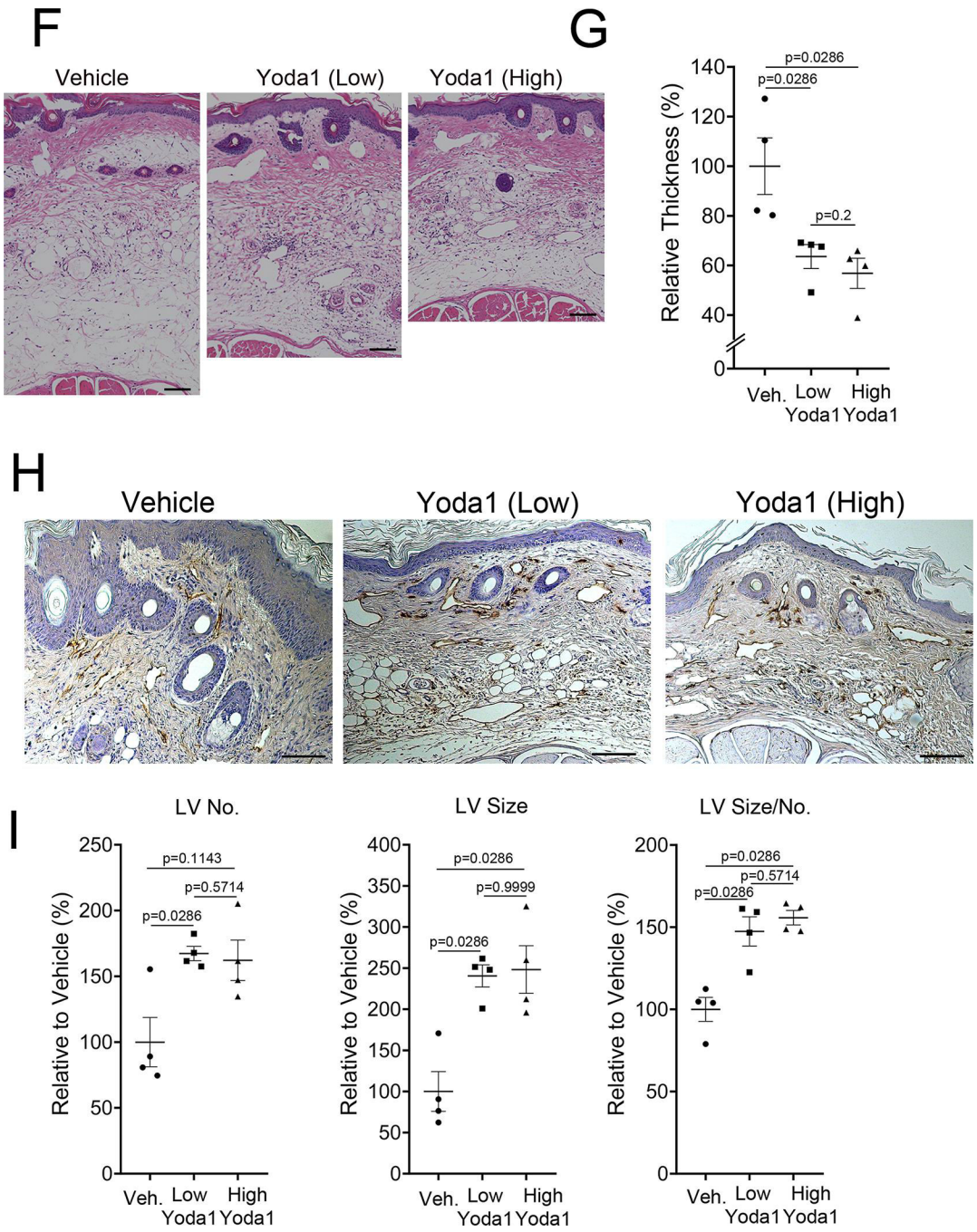

Figure 8. Yoda1 Prevents Lymphedema Formation in Mouse: Potential Therapeutic Efficacy

(**A**) Experimental tail lymphedema images demonstrating a therapeutic efficacy of Yoda1. The tail lymphedema model was introduced to adult Prox1-EGFP mice. Vehicle control (n=18) or Yoda1 at low (n=15, 71 μg/kg/day) or high (n=13, 213 μg/kg/day) was i.p. injected daily from post-operation day (POD) 0 for 35 days. (**B**) Graph showing the degree of lymphedema by charting percent changes in the tail volume of each group over 35 days. Tail volume was measured weekly. (**C**) ICG-based lymphangiography assessing lymphatic function. At POD 35, ICG was injected at the tip of the tail, and fluorescent images were

captured over 96 hours. Representative images are shown after 3 min., 24 hours, and 48 hours post-ICG-injection. (**D**) Graph showing the rate of ICG clearance reflecting lymphatic function. ICG fluorescence intensity was measured from captured images. N = 10/group. $p < 0.001$ from 4 hours to 96 hours post-ICG-injection. Scale bars: 5 mm in panels A and C (**F**) H&E staining of paraffin sections prepared from an immediately distal area of the surgery site. (**G**) Thickness of the subcutaneous area was measured, and the relative values are charted. (**H**) Anti-Lyve1 immunohistochemistry visualizing lymphatic vessels (n=4 mice per group). (**I**) Graphs showing relative lymphatic vessel number (LV No), vessel size, and size/number (n=4 mice per group). Vessel size is determined by measuring their circumferences. Scale bars: 100 μm in **F** and **H**. Statistics: ANCOVA (**B** and **D**), Mann-Whitney *U* test (**G** and **I**).